

Androgen receptor signaling blockade enhances NK cell-mediated killing of prostate cancer cells and sensitivity to NK cell checkpoint blockade

Maximilian Pinho-Schwermann^{1,4}, Benedito A. Carneiro³⁻⁵, Lindsey Carlsen¹⁻⁴, Kelsey E. Huntington¹⁻⁴, Praveen R. Srinivasan^{1,4}, Andrew George^{1,4}, Vida Tajiknia^{1,4}, William MacDonald^{1,4}, Connor Purcell^{1,4}, Lanlan Zhou¹⁻⁴, Andre De Souza³⁻⁵, Howard P. Safran³⁻⁵, Wafik S. El-Deiry¹⁻⁵

1 Laboratory of Translational Oncology and Experimental Cancer Therapeutics, Department of Pathology and Laboratory Medicine, The Warren Alpert Medical School, Brown University, Providence, RI 02903, USA

2 Graduate Program in Pathobiology, The Warren Alpert Medical School, Brown University, Providence, RI 02903, USA

3 Joint Program in Cancer Biology, Brown University and The Lifespan Health System, Providence, RI 02903, USA

4 Legorreta Cancer Center at Brown University, The Warren Alpert Medical School, Brown University, Providence, RI 02903, USA

5 Hematology-Oncology Division, Brown University and The Lifespan Cancer Institute, Providence, RI 02903, USA

Running title: Androgen blockade enhances NK cell immune checkpoint inhibition.

Keywords: prostate cancer, androgen signaling, NK cells, immune checkpoint inhibitor, NKG2a, monalizumab.

Corresponding author:

Wafik El-Deiry, MD, PhD, FACP

70 Ship Street, Box G-E5

Providence, RI, USA RI

Phone Number: 401-863-9687; Fax Number: 401-863-9008

Email: wafik@brown.edu

Abstract

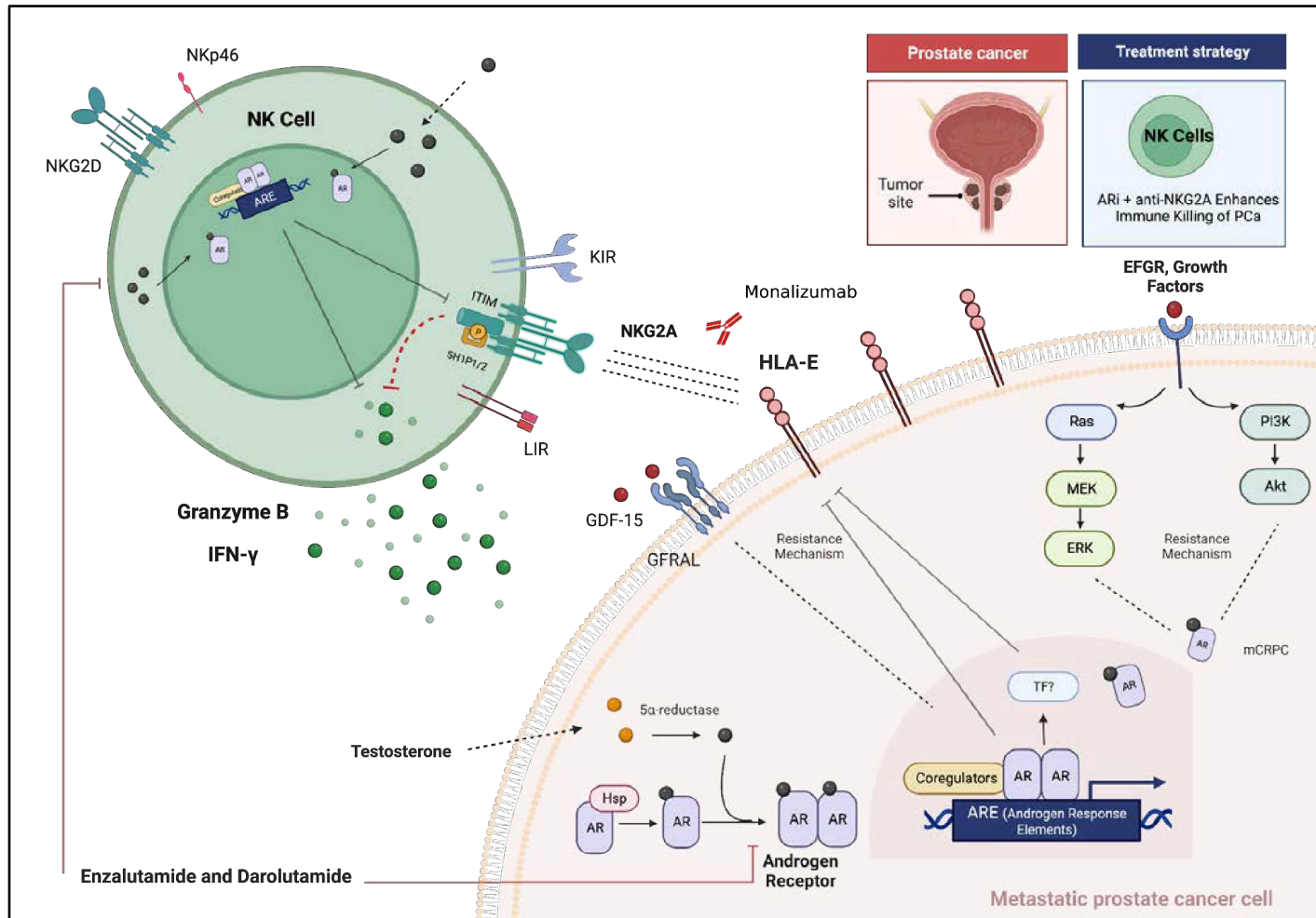
Background: The blockade of the androgen receptor (AR) pathway is an effective treatment for prostate cancer (PCa), but many patients progress to metastatic castration-resistant prostate cancer (mCRPC). Therapies for mCRPC include AR inhibitors (ARI), chemotherapy, PARP inhibitors, and radioligands. Checkpoint inhibitor activity is limited to a small subset of MSI-H mCRPC. AR signaling modulates CD8+ T cell function, but its impact on NK cell (NKc) cytotoxicity is unknown. We investigated the effect of ARI on NKc activation, cytokine secretion, expression of inhibitory receptor NKG2A, and killing of PCa cells *in vitro*.

Methods: PCa cell lines (LNCaP, 22Rv1 [ARv7 mutation], DU145[AR-], PC3 [AR-]) were co-cultured with NK-92 cells and treated with ARI (enzalutamide [enza] and darolutamide [daro]) or in combination with anti-NKG2A antibody monalizumab. Immune cell-mediated tumor cell killing assays and multiplexed cytokine profiling were performed. NKc expression of NKG2A and PCa cells expression of HLA-E were investigated by flow cytometry. The AR-negative cell lines (PC3 and DU145) were stably transduced with a functional AR pathway to evaluate the modulation of HLA-E by AR. The activation status of peripheral blood NKc isolated from patients with PCa before and post-initiation of androgen deprivation therapy (ADT) was investigated by flow cytometry.

Results: ARI significantly increased immune-mediated NK-92 cell killing of PCa cells independent of their sensitivity to androgen signaling. Cytokine analysis revealed that ARI-induced NKc activation is mediated by IFN- γ and TRAIL, as confirmed by blocking antibodies. ARI increased NKG2A expression in NK cells. Immune killing of PCa cells was enhanced with the combination of ARI and monalizumab. ARI also increased the expression of HLA-E, the ligand of the inhibitory NKG2A receptor, on PCa cell lines. Using AR-negative cell lines (PC3 and DU145) and stable transduction of AR, we demonstrate that androgen signaling regulates HLA-E expression. HDAC inhibitors (vorinostat and panobinostat) did not alter the androgen-induced expression of HLA-E in PCa cells. Mirroring the results from NK-92 cells, ADT also activated peripheral blood NK cells isolated from patients with metastatic PCa.

Conclusions: ARI activates NK cells through upregulating IFN- γ and TRAIL and promotes the killing of PCa cells. This enhanced cytotoxic killing of PCa cells is augmented by monalizumab. ARI upregulates PCa cell's expression of HLA-E, suggesting a mechanism suppressing the innate immune response against PCa. These results support novel therapeutic strategies for PCa targeting NK activation with the combination of ARI and monalizumab.

Graphical Abstract: Androgen receptor signaling blockade enhances NK cell-mediated killing of prostate cancer cells and sensitivity to NK cell checkpoint blockade. Nonetheless, ARI can potentially upregulate an NK cell inhibitor ligand (HLA-E), thus suppressing NK cell killing of PCa. This regulation is dependent on a functional AR signal on tumor cell lines. Adding an anti-NKG2a-HLA-E mAb with ARI further enhances the NK cell-mediated killing of PCa.



Introduction

Prostate cancer (PCa) is the most common cancer in men and ranks second as cancer-related death in the United States in men [1]. Although most patients present with localized disease, progression to metastatic disease and its management remains a significant clinical challenge. Blockade of androgen receptor (AR) signaling is essential for treating PCa. Most patients with advanced disease progress to metastatic castration-resistant prostate cancer (mCRPC), associated with a median OS of 4-5 years [2]. Standard treatments for mCRPC include AR-targeted agents (i.e., enzalutamide, darolutamide, apalutamide), the CYP17 inhibitor abiraterone, chemotherapy (docetaxel, cabazitaxel), Lutetium 177-PSMA-617, and PARP inhibitors. Although the first therapeutic cancer vaccine approved more than a decade ago targeted prostate tumors (sipuleucel-T), the clinical efficacy of immunotherapy for treating PCa remains limited, with poor responses to checkpoint inhibitors as monotherapy [3]. PCa tumors display an immunosuppressive tumor microenvironment mediated by reduced expression of human leucocyte antigen (HLA) surface expression, decreased neoantigen expression, phosphatase and tensin homolog (PTEN) protein loss, and dysfunction of interferon (IFN) type I signaling [4-5]. These factors contribute to low response rates to checkpoint inhibitors in most cases of mCRPC, except for MSI-H tumors and those with CDK12 mutations [6-7]. Novel immunotherapy strategies represent an active area of research to overcome immunologically cold PCa.

Emerging results suggest that AR signaling modulates the immune response by inhibiting CD8 and CD4 T cells [8]. AR blockade enhances CD8+ T cell function and sensitizes tumors to PD-1 checkpoint inhibitors in animal models of prostate cancer [8-9]. Androgen signaling in T cells suppresses IFN- γ secretion *in vitro* and contributes to T cell exhaustion. These effects were reversed with AR blockade and contributed to PSA and tumor responses observed among patients with mCRPC treated with pembrolizumab (anti-PD-1) and enzalutamide in a clinical trial [10]. In addition, gene expression analysis of CD4+ T cells isolated from castrated mice identified protein tyrosine phosphatase non-receptor type 1 (Ptpn1) as a mediator of androgen-induced suppression of CD4+ T-cell differentiation [11,12,13]. Up-regulation of interferon regulatory factor-1, 3, and 7 (IRF-1,3 and 7) and STAT4 in CD4+ T cells from mice were also observed, suggesting that androgens could alter the IL-12-induced STAT4 phosphorylation and impair CD4+ T cells. These results highlight the role of AR signaling in CD8 and CD4 T cells, but the impact on NK cells has yet to be elucidated.

We investigated the effect of AR inhibitors enzalutamide (enza) and darolutamide (daro) on NK cell activation *in vitro* using co-culture experiments of immune cells, PCa cell lines, and patient--

derived immune cells. The results revealed that AR inhibitors enhance the immune killing of prostate cancer cells by a mechanism mediated by IFN- γ and TRAIL with augmentation when combined with monalizumab, an inhibitor of the NK cell receptor NKG2A. We also revealed the androgen-dependent modulation of HLA-E in PCa cells as a potential mechanism to suppress the innate immune response and protect PCa cells from NK cell killing. These results support the development of novel immunotherapy approaches in prostate cancer to promote the activation of NK cells with ARi and monalizumab, among other potential NK cell-based therapeutics.

Materials and Methods:

Cell lines and culture conditions

Prostate cancer cell lines (obtained from ATCC) included PC3, DU145, LNCaP, and 22Rv1. Cells were grown in RPMI 1640 medium (Cytiva HyClone SH30027LS) supplemented with 10% fetal bovine serum, 1% sodium pyruvate, 1% GlutaMAX, and 1% penicillin/streptomycin at 37°C, 5% CO₂. Cells were trypsinized (0.25% trypsin) upon flask confluence and tested for Mycoplasma every 6 months. Even though 22Rv1 constitutively expresses the androgen receptor, it is resistant to androgen blockade due to a splice-site mutation (AR-V7) [14].

NK cell line NK-92 was obtained from ATCC (RRID: CVCL_2142). The cell line was grown in alpha-MEM medium supplemented with 10% FBS, 1% sodium pyruvate, 1% Glutamax, 1% penicillin/ streptomycin, 0.1 mM of 2-mercaptoethanol, 12.5% of heat-inactivated horse serum, 1% Non-Essential Amino Acids (NEAA), 1% folic acid and 20 mM myoinositol at 37°C, 5% CO₂. NK-92 cells were kept at 4-5 x 10⁵ cells/ml seeding concentration and supplemented with 100 IU/ml of recombinant human IL-2 every two days. Cells were passaged using Ficoll PM400, sodium diatrizoate, and disodium calcium EDTA solution (Ficoll-Paque PLUS Cytiva 17-1440-02) every 10-14 days and up to 72h before plating/experiments.

Western blot analysis

Anti-apoptotic proteins and androgen receptor expression in prostate cancer cell lines and immune cells (NK-92) were examined using a western blot. A total of 1x10⁵ cells were plated and incubated in a 6 or 12-well plate (CELLTREAT 229111 and 229105) for 24 hours to allow the cells to adhere (tumor cells). Treatment conditions were added after cell adhesion or in conjunction with NK cells when these were analyzed. Cells were harvested and lysed using RIPA buffer containing protease inhibitor (Cell Signaling Technology 9806S) and phosphatase inhibitor (PHOSS-RO Roche 4906845001). Denaturing sample buffer was added, and samples were boiled at

95°C for 10 minutes and an equal amount of protein lysate (10-20 ug) was electrophoresed through 4–12% SDS-PAGE gels (Invitrogen) and then transferred to PVDF membranes. The membrane was blocked with 5% milk in 1X TTBS and incubated overnight with the appropriate primary antibody (Cell Signaling c-IAP2 58C7 Rabbit mAb #3130; Cell Signaling XIAP Antibody #2042; Cell Signaling Mcl-1 (D2W9E) Rabbit mAb #94296; Cell Signaling Survivin (71G4B7) Rabbit mAb; Cell Signaling Ran Antibody #4462; Cell Signaling PARP 9542T mAb; Cell Signaling Bcl-2 Antibody #2876; Cell Signaling Bcl-xL (54H6) Rabbit mAb; Sigma Aldrich Monoclonal Anti-β-Actin antibody #A5441; Cell Signaling Androgen Receptor (E3S4N) Rabbit mAb (Carboxy-terminal Antigen) #70317). The primary antibody membranes were incubated in the appropriate HRP-conjugated secondary antibody (either mouse, Thermo Scientific #31430, or rabbit, Thermo Scientific #31460) for two hours. The levels of antibody binding were detected using ECL western blotting detection reagent and the Syngene imaging system.

Establishing IC50 doses

PCa cells were plated at a density of 5×10^3 cells per well of a 96-well plate. Cells were treated with doses ranging from 0-250 μM of anti-androgens enzalutamide and darolutamide. For NK cell viability assays, 5×10^3 cells were plated in a 96-well plate, and viability (72h) was measured using a CellTiterGlo assay. Bioluminescence imaging was measured using the Xenogen IVIS imager. IC50 doses were determined based on the dose-response curve collected from the data. Concentrations used in the experiments were correlated with those findings, matched with literature reports, and clinical correlation when possible.

Co-culture assays

Prostate cancer cell lines were dyed with the blue CMAC live-cell dye (Thermo Fisher Scientific #C2110, per manufacturer protocol). Blue-fluorescent cancer cells were plated at a density of 10,000 cells per well of a 48-well plate. NK-92 cells were dyed with green CMFDA (Cayman Chemical Company #19583, per manufacturer protocol). Green-fluorescent NK-92 cells were added to the blue-fluorescent cancer cells at a 1:1 ratio. Enzalutamide (10 μM), darolutamide (20 μM), and 1 μM ethidium homodimer (EthD-1) were added at the same time as the NK cells. After 24 hours of co-culture, images of live cancer cells, live NK cells, and dead cells were taken using a fluorescent microscope. The co-culture experiments were run with internal control conditions and as a single treatment. Normalization was performed after analysis to take baseline death conditions into each experiment run. To optimize the high output of these experiments, a subset of co-cultures were performed using the ImageXpress® Micro Confocal High-Content Imaging. This analysis

maintained the experiment conditions, drug concentrations, and the dyeing process. When GFP-labeled tumor cells were used for culture assays, they were added in a 1:1 ratio. Cell adhered over 24h, and when patient-derived NK cells were added, a control well was trypsinized, and cells resuspended and counted to adjust a 1:1 ratio before treatment addition. The experiments with blocking antibodies were performed using the ImageXpress system. TRAIL blocking ab was purchased from Santa Cruz TRAIL Antibody (RIK-2): sc-56246, and IFN gamma blocking Monoclonal Antibody (NIB42, #6-7318-81) was purchased from Thermo Fisher. The blocking mAb was added when NK cells were combined with tumor cells.

Statistical analysis

Live cancer cells, NK cells, and dead cells were quantified using FIJI (Fiji Is Just ImageJ) software for images derived from fluorescent co-culture images. Images from the ImageXpress system were quantified using MetaXpress cytoplasmic/nuclear staining software. The percent of dead tumor cells in each well was quantified, and this percentage was normalized by subtracting baseline death from cancer cell-only wells, NK cell-only wells, or both. A two-way ANOVA was used to calculate the interaction effect between drug treatment and NK cells.

In groups with a significant interaction effect, data was further normalized in the cancer cell + NK cells + drug treatment well by subtracting out death in the cancer cell + drug well. A one-way ANOVA and multiple comparison analysis with subsequent t-tests were used to calculate the statistical significance of the difference between this group and the cancer cell + NK cell well. GraphPad Prism Version 9.5.1 was used for statistical analysis.

Generation of stably expressing GFP cell lines, Androgen Receptor, and Reporter inducible system.

GFP Positive Cell Line Production:

The prostate cancer cell lines (PC3, DU145, LNCaP, and 22Rv1) were seeded at 50% confluence in a 12-well tissue culture plate and adhered overnight. Then, they were transduced with lentivirus containing pLenti_CMV_GFP_Hygro [pLenti CMV GFP Hygro (656-4) was a gift from Eric Campeau & Paul Kaufman (Addgene viral prep #17446-LV)] at a multiplicity of infection of 10 for 48 hours before washing with PBS and replacing with fresh medium. The cells were then sorted for GFP-positivity using a BD FACSAria™ III Cell Sorter (RRID: SCR_016695).

Plasmid handling:

Agar stabs with plasmid-containing bacteria were obtained from Addgene. Bacteria were streaked onto LB agar dishes with 100 µg/mL ampicillin and grown at 30°C for 24 hours. Single colonies were then Midi-prepped (QIAGEN Plasmid Plus Midi Kit, 12943) according to the manufacturer's protocol. The plasmid sequence was verified by whole-plasmid sequencing (Plasmidsaurus) using Oxford Nanopore technology.

Lentivirus production:

Five million HEK293T cells (ATCC CRL-3216) were seeded in a 10 cm tissue culture dish with 6 mL of antibiotic-free DMEM with 10% FBS (ATCC 30-2020) and adhered overnight. They were then transfected using 50 µL of Lipofectamine 2000 (Thermo Fisher 11668019), 10 µg of transfer plasmid [either pLENTI6.3/AR-GC-E2325 (Addgene 85128, pLENTI6.3/AR-GC-E2325 was a gift from Karl-Henning Kalland) or ARR3tk-eGFP/SV40-mCherry (Addgene 132360, ARR3tk-eGFP/SV40-mCherry was a gift from Charles Sawyers)], 5 µg of pMDLg/pRRE (Addgene 12251, pMDLg/pRRE was a gift from Didier Trono), 5 µg pRSV-Rev (Addgene 12253, pRSV-Rev was a gift from Didier Trono), and 2.5 µg of pMD2.G (Addgene 12259, pMD2.G was a gift from Didier Trono). After 16 hours, the medium was exchanged. Forty-eight hours after transfection, the medium was harvested, centrifuged at 500g for 5 minutes, and the supernatant was sterile-filtered through a 0.45 µm polyethersulfone syringe filter (Millipore SLHPR33RS). The supernatant was then stored at -80°C for future use.

Lentivirus Transduction for pLENTI6.3/AR-GC-E2325 and ARR3tk-eGFP/SV40-mCherry:

PC3 and DU145 cell lines were seeded at 50% confluence in a 12-well tissue culture plate and allowed to adhere overnight. Varying volumes of viral supernatant were added to each well for 48 hours. Wells were then washed with PBS and replaced with fresh medium. For pLENTI6.3/AR-GC-E2325, cells were selected with 2.5 µg/ml (PC3) and 5 µg/m (DU145) of blasticidin (InvivoGen ant-bl-1) for 7-9 days. For ARR3tk-eGFP/SV40-mCherry, cells were sorted for mCherry-positivity using a BD FACSAria™ III Cell Sorter (RRID: SCR_016695).

Isolation of Human NK Cells

NK cells were isolated from patients harboring metastatic castration-sensitive prostate cancer using the MojoSort™ Human NK Cell Isolation Kit (#480053). Patients signed informed consent for IRB-approved research protocol number 2055-13, allowing the collection of peripheral blood samples. Cells were isolated from patients using a density-dependent methodology, Ficoll PM400, sodium diatrizoate, and disodium calcium EDTA solution (Ficoll-Paque PLUS Cytiva

17-1440-02). Following the suggested protocol from the manufacturer of negative selection sorting, non-natural killer cells were depleted by incubating the patient's whole PBMCs sample with the biotin antibody cocktail (BioLegend 480053) followed by incubation with magnetic Streptavidin Nanobeads. The magnetically labeled fraction (non-NK cell population) was retained using a magnetic separator (BioLegend 480019). The untouched NK cells (CD56+, CD3-) were collected, and the purity of isolation was determined by flow cytometry using anti-CD56 (BioLegend 362503). NK isolated cell populations were only kept in NK cell medium (see methods above) and further plated for experiments if the purity of the sample for CD56+ was above 98%.

Cytokine Analysis

A total of 3×10^5 PC3, LNCaP, 22Rv1, and DU145 cells were plated per well of a 24-well plate and treated for 5-7 days with 15 nM of DHT (dihydrotestosterone) before ARi were added. A total of 2×10^5 of NK-92 were incubated in 15 nM of DHT for 72h before enza or darolutamide treatment. The medium was collected 24 hours after treatment and stored at -80°C until readout. Samples were shipped to Brown University to run them in biological duplicate on a Luminex 200 Instrument (R&D LX200-XPON-RUO), which captures cytokines on magnetic antibody-coated beads and measures cytokine levels using a system based on the principles of flow cytometry (see <https://www.luminexcorp.com/luminex-100200/#overview> for more information). A custom 52- 52- cytokine panel was split into 34-plex and 18-plex assays (R&D LXSAHM) and was run on the Luminex 200 instrument according to the manufacturer's protocol.

Flow Cytometry

PCa cells were plated at a density of 3×10^5 cells per well of a 6-well plate and adhered overnight. In experiments where the treatment conditions included enza and darolutamide, cells were kept in culture in the presence of DHT (20-30 nM) for at least 72h. After treatment, cells were trypsinized, stained, and incubated (Cell Staining Buffer SouthernBiotech #0225-01S) with the corresponding antibody for 45-60 min at 4°C. Viability dye was added with each run. NK-92 cells and patient-derived cells were stained similarly. Markers used for experiments included: Thermofisher HLA-E Monoclonal Antibody (3D12HLA-E), Alexa Fluor™ 488, eBioscience™, CD274 (PD-L1, B7-H1) Monoclonal Antibody (MIH1), eFluor™ 450, eBioscience™, Cell Signaling PD-1 (D4W2J) XP® Rabbit mAb, SYTOX™ Orange Dead Cell Stain, for flow cytometry, BioLegend APC anti-human CD159a (NKG2A) Antibody #375108, BioLegend APC anti-human CD69 Antibody #310909, BioLegend Alexa Fluor® 647 anti-human CD137 (4-1BB) [4B4-1] #309823. For staining of the patient-derived PBMCs and subsequent NK cell characterization,

the following antibodies were used: BioLegend Anti-Perforin Mouse Monoclonal Antibody (PerCP Cy5.5®, clone: dG9) #308113, BioLegend Anti-Granzyme B Mouse Monoclonal Antibody (FITC, clone: GB11) #515403, BioLegend Anti-CD56 Mouse Monoclonal Antibody (Alexa Fluor® 700, clone: 5.1H1) #362521, and BioLegend (PE anti-human CD45 Antibody) #304008.

Results

Androgen receptor inhibitors enhance NK cell killing of prostate cancer cells *in vitro*

Prostate cancer cell lines (22Rv1, LNCaP, PC3, and DU145) were treated with DHT (15-30 nM), and immune cells were added 24 hrs later at a 1:1 ratio. They were co-treated with enzalutamide (15 μ M) or darolutamide (20 μ M) for 48h. Doses of AR inhibitors (ARI) used in the co-culture experiments were based on our findings (**Supp. Fig. 1**) and previous IC50 experiments [15,16,17]. These doses did not impact NK or PCa cell viability (**Supp. Fig. 1**).

ARI treatment of co-cultures with PCa plus NK-92 cells significantly increased immune-mediated PCa killing within 24 hours independent of PCa cell line AR status and sensitivity to ARI (**Fig. 1A-D**). Enzalutamide significantly increased NK cell-mediated tumor killing of LNCaP in 24 hours (cell death rate: 15.6% \pm 3.9 (control[C]) vs 48.3% \pm 8.3 (enza); p<0.0001). This effect with enzalutamide was also observed in ARI-resistant cell lines PC3 (3.8% \pm 1.27 (C) vs. 11.05 \pm 4.6 (enza); p<0.0017), 22Rv1 (17.07% \pm 3.35 (C) vs 52.67 \pm 8.96 (enza); p<0.0001), and DU145 (13.45% \pm 2.37 (C) vs 34.8 \pm 4.92 (enza); p<0.001). The enhancement of NK cell-mediated killing was also demonstrated with another ARI, darolutamide (daro; **Fig. 1**), and the maximal effect was observed within 24-30h. Cytokine analysis was performed to investigate the activation phenotype of NK cells when treated with ARI.

The ARI immune enhancement and killing of PCa cell lines by NK cells is dependent on IFN- γ and TRAIL

The NK-92 cell line was treated with 10 nM of DHT for 72h before treatment with enza or daro, and cytokines were measured in the culture supernatant. The secretion profile was assessed in monoculture conditions without the PCa cell lines (**Fig. 2A**).

Daro and enza increased NK-92 cell secretion of IFN- γ ([C]: 12.98pg/ml \pm 3.4; Enza: 48.88 pg/ml \pm 3.18; Daro: 45.6pg/ml \pm 9.4, p=0.01) and granzyme B ([C]: 676.6pg/ml \pm 36.2; Enza: 1027 pg/ml \pm 105.5; Daro: 1599pg/ml \pm 118.6, p<0.001), and decreased the secretion of the immunosuppressive cytokine IL-10 ([C]: 27.3pg/ml \pm 4.16; Enza: 16.6 pg/ml \pm 2.01; Daro:

15.24pg/ml \pm 1.48, p=0.04) (**Fig. 2B1-6**). These results supported the role of ARI inducing NK activation and enhancing cytotoxic function through IFN- γ secretion.

To investigate the role of IFN- γ in mediating this ARI-induced enhancement of NK cell killing, IFN- γ -neutralizing monoclonal antibody (mAb) (10 ug/ml) was combined with ARI in co-culture experiments. Doses of the α -IFN- γ mAb were based on previous experiments and co-culture assays [18,19,20]. Blocking IFN- γ reversed the immune enhancement effect of enzalutamide (**Fig. 2C- D**). Based on the upregulation of soluble ligands TRAIL-R2 and R3 by ARI on our cytokine analysis (data not shown), we investigated the dual blockade of IFN- γ and TRAIL with RIK-2 (TRAIL-CD253 neutralizing mAb).

Treatment of PCa and NK cells in the presence of enza, α -IFN- γ mAb, and RIK-2 reduced the NK cell-mediated killing of PCa cells (**Fig. 2C-D**). In the presence of enzalutamide treatment, the blockade of TRAIL diminished the immune enhancement killing, but not to the same degree as IFN- γ mAb blockade alone (**Fig. 2C-D**). The dual blockade, targeting TRAIL and IFN- γ , diminished NK cell PC cell killing almost entirely, even in the presence of ARI (**Fig. 2C-D**).

The surface expression of the NK cell activation markers CD69 and CD137 were also evaluated following the treatment of NK cell monocultures with ARI (**Fig. 2F-G**). Enza and daro increased the expression of CD69 and CD137 (CD69 [C]:77.7% \pm 4.75, enza: 87.4% \pm 1.4, daro: 88.63% \pm 1.94, p=0.009; CD137 [C]:35.1% \pm 4.77, enza: 61.54% \pm 12, daro:64.87% \pm 7.96, p=0.01).

ARI modulates apoptotic and antiapoptotic proteins as well as pro and antitumorigenic cytokines in PCa cell lines

We investigated the effects of ARI on PCa cells' expression of Bcl-2 proteins and cytokine secretion to assess a possible priming effect of treatment, making these cells susceptible to NK cell killing. Enzalutamide (5, 10, and 15 μ M) and darolutamide (10, 20 μ M) reduced the expression of the X-linked inhibitor of apoptosis (XIAP) in DU145, 22Rv1, and LNCaP cell lines (**Fig. 3A**). The PC3 cell line expressed lower levels of XIAP at baseline, which did not change with treatment. The reduced expression of XIAP was more pronounced with darolutamide than enzalutamide. Both ARI also reduced the expression of c-IAP2 (DU145 cells and LNCaP) and Bcl-XL (22Rv1). Survivin levels decreased with treatment only in LNCaP. There was no significant change in the expression of the antiapoptotic protein MCL-1 in any cell lines with treatment (**Fig. 3A-B**). These results suggest that ARI modulate anti-apoptotic proteins in both androgen-sensitive and resistant prostate cancer cell lines, potentially increasing their susceptibility to immune-mediated killing as

previously shown for AR-sensitive tumor cells [21]. Nevertheless, these changes were not consistent in all PCa cell lines, and some were of limited magnitude, making the interpretation of their functional impact on susceptibility to NK cell killing difficult.

We then investigated the cytokine profiles of prostate cancer cell lines after treatment with ARi. Each cell line was treated with 10 nM of DHT for at least 72 hours before treatment with enzalutamide or darolutamide. The results are depicted in **Fig. 3C-D** and **Supp. Fig. 3**. Treatment of PCa cell lines with enzalutamide and darolutamide for 24h increased the secretion of immune-activating cytokines such as IL-2 and reduced the secretion of pro-tumorigenic and immunosuppressive cytokines such as VEGF, M-CSF, IL-8, CXCL10 and GDF-15 (**Supp. Fig. 3**). Additionally, DU145, 22Rv1, and PC3 cell lines had upregulation of IFN- γ . ARi downregulated soluble FasL and increased TRAIL-R2 and R3. Upregulation of GDF-15 by ARi was limited to ARi-resistant prostate cells (PC3, DU145, and 22Rv1). GDF-15 is implicated in the immunosuppressive prostate cancer TME and the progression of benign prostate hyperplasia to adenocarcinoma [18, 22].

Blocking the NK cell receptor NKG2A with monalizumab potentiates the ARi-induced immune-mediated killing of PCa cells

To evaluate a strategy to potentiate NK cell killing induced by ARi, co-culture experiments of PCa and NK cells were performed with enzalutamide combined with monalizumab, an NKG2A blocking mAb. Monalizumab significantly increased enzalutamide-induced immune enhancement irrespective of the ARi sensitivity of PCa cell lines. (**Fig. 4A-B**; LNCaP: [C] $15.89\% \pm 3.56$, enza: $35.32\% \pm 1.09$, monalizumab: $19.89\% \pm 2.4$, enza+monalizumab: $45.97\% \pm 4.04$, $p=0.001$; 22Rv1: [C]: $14.23\% \pm 2.03$, enza: $34.84\% \pm 1.96$, monalizumab: $18.29\% \pm 2.5$, enza+monalizumab: $46.916\% \pm 2.4$, $p=0.001$). Monalizumab as a single agent did not enhance NK cell killing (**Fig. 4A-B**) or impact PCa or NK cell viability (data not shown).

To validate an additive effect of ARi and monalizumab enhancing NK cell cytotoxicity, we performed a co-culture assay with GFP-labeled PCa cell lines (including ARi-sensitive LNCaP and ARi-resistant PC3) and patient-derived NK cells. The NK cells were negatively selected from whole blood from patients with metastatic prostate cancer before initiation of androgen deprivation therapy. The addition of enzalutamide or darolutamide enhanced the cytotoxicity of NK cells, and the combination of ARi with monalizumab potentiated immune killing (**Fig. 4C-D**). Even though this effect was evident irrespective of the AR status of the cell line, the ARi-sensitive cell line, LNCaP, displayed greater sensitivity to the addition of monalizumab in combination with enzalutamide or darolutamide (**Fig. 4C-D**).

To investigate the effects of androgen deprivation therapy (ADT) on the activation of peripheral blood NK cells, blood samples were collected from patients diagnosed with castration-sensitive metastatic prostate cancer before initiation of ADT and approximately 26 days later when patients had achieved castration levels of testosterone (median time between sample collections: 26.3 ± 8.7 days). Patient characteristics are summarized in **Fig. 7A**. Per standard of care, ADT was implemented with the administration of luteinizing hormone-releasing hormone (LHRH) agonists (e.g., leuprolide) or antagonists (e.g., degarelix). Patient-derived NK cells were co-cultured with PCa cells in a 1:1 ratio for 48h and then analyzed by flow cytometry. After ADT, the patients displayed a greater number of granzyme B+ NK cells (pre-ADT: 20.53 ± 2.77 ; post-ADT: 37.24 ± 6.9 ; $p=0.0017$), as well as perforin+ NK cells (pre-ADT: 4.26 ± 0.92 ; post-ADT: 54.47 ± 6.47 ; $p<0.001$). The double-positive NK cell population (positive for granzyme B and perforin) also increased after ADT (pre-ADT: 3.54 ± 0.42 ; post-ADT: 38.15 ± 7.96 ; $p=0.001$) (**Fig. 7C-D**).

Androgen receptor blockade upregulates HLA-E in androgen-signaling sensitive PCa cells but not in androgen-independent ones.

The effect of ARi on the NKG2A ligand, HLA-E, was investigated by flow cytometry on PCa cells treated with enza and daro. ARis increased the surface expression of HLA-E in LNCaP ([C]: $28.57\pm2.4\times10^3$, enza: $37.38\pm1.7\times10^3$ and daro: $39.47\pm3.39\times10^3$, $p=0.004$) (**Fig. 5A**), and did not affect HLA-E expression of ARi-resistant cell line 22Rv1 ([C]: $34.76\pm5.1\times10^3$, enza: $41.14\pm7.6\times10^3$ and daro: $30.5\pm2.69\times10^3$, $p=0.14$) (**Fig. 5B**).

To evaluate the modulation of the androgen receptor and tumor HLA-E expression, we stably transduced AR negative cell lines PC3 and DU145 with an Androgen Response Element (ARE) GFP reporter (**Fig. 5H**). After stably transducing these reporter-containing cells with an AR receptor (**Fig. 5H**), the transduced AR activity was confirmed by treating these AR+-constructed cell lines with DHT in different concentrations for 72h. The expression and targeting of ARE were confirmed by increased expression of GFP+ cells (**Fig. 5H**). This system allowed us to evaluate AR-dependent signaling pathways. Using AR+ constructed cell lines, PC3 and DU145, we sought to determine the dependence of HLA-E expression and possible modulation by AR. As seen previously by the ARi resistant 22Rv1 cell line, non-AR-transduced cell lines did not alter their HLA-E expression (PC3 [C]: 11.41 ± 3.16 , DHT: 11.28 ± 2.19 , Daro: 15.47 ± 1.5 , $p=0.12$, DU145 [C]: 2.06 ± 0.61 , DHT: 1.84 ± 0.22 , Daro: 1.23 ± 0.6 , $p=0.11$). Nevertheless, the AR-transduced cells showed decreased HLA-E expression upon ARi treatment, similar to what was seen with the AR-

sensitive LNCaP cell line described previously (**Fig. 5C-F**). This could be a possible AR-dependent mechanism by which the treatment with ARi in combination with an NKG2A blocking strategy yielded a better killing profile in the presence of NK cells than the AR-insensitive ones. Although potential therapies targeting immune enhancement are being explored, the expression of exhaustion markers such as PD-1, NKG2A, and potential engaging ligands that diminish their cytotoxic function limits their application. Exploring these factors with new combination approaches, such as ARi and anti-NKG2A, and understanding the modulation of its targets upon treatment is key in overcoming immune-resistant scenarios, especially in prostate cancer.

To explore a potential epigenetic regulation of HLA-E surface expression by androgen regulation, the HLA-E expression was evaluated on the PC3 and the AR-responsive cell line (LNCaP) after DHT treatment with and without pan-HDAC inhibitors vorinostat and panobinostat. Both cell lines were kept in culture for at least five days in the presence of 30 nM of DHT before the experiments (**Fig. 6**). The AR negative cell line, PC3, did not alter its surface expression of HLA-E upon treatment of DHT. The addition of HDACi did not change its surface expression (**Fig. 6A**). Experiments were conducted with noncytotoxic doses of vorinostat (0.3 μ M) and panobinostat (3nM), as depicted by supplementary **Fig. 3**. Interestingly, the expression of HLA-E on the AR responsive cell line (LNCaP) did not change significantly upon DHT treatment if cells were further treated with HDACi for 48h (**Fig. 6B**). These results suggest that HLA-E regulation in the ARi-sensitive cell lines partly depends on epigenetic regulation.

Discussion

Our results demonstrate that blockage of androgen signaling activates NK cells *in vitro* and enhances the killing of PCa cells in co-culture experiments. The AR inhibitors enzalutamide and darolutamide increased NK cell secretion of cytokines IFN- γ and TRAIL that mediated PCa killing. The blockade of IFN- γ inhibited this effect significantly, and the dual blockade of IFN- γ and TRAIL had further additive effects. Monalizumab, a monoclonal antibody blocking the immune inhibitory receptor NKG2A on NK cells, potentiated the NK cell cytotoxicity induced by ARi. The AR inhibitors also modulated PCa cells by decreasing the secretion of pro-tumorigenic factors (i.e., IL-4, TNF-a, VEGF, MIF, M-CSF, and GM-CSF) and downregulating anti-apoptotic proteins (XIAP, c-IAP2, and Bcl-XL). Our results also reveal a novel androgen-driven regulation of HLA-E expression in PCa cells. HLA-E is a nonclassical HLA class I molecule and the main ligand of the NKG2A receptor [23]. HLA-E is frequently overexpressed in tumors and contributes to immune escape in the TME by inhibiting NK cells and NKG2A-expressing CD8 T cells [24]. ARi-induced HLA-E expression in prostate cancer cells can protect them from NK lysis, contribute to a cold

immune environment, and might represent a mechanism of resistance enabling the persistence of prostate cancer cells during treatment with AR inhibitors as well as ADT, a finding with significant clinical importance for the treatment of prostate cancer.

Our findings showing the immune-modulatory role of androgen signaling on NK cells and complement results describing the effect of ADT and AR blockade on T cell function. Building upon a clinical trial investigating the combination of anti-PD1 (pembrolizumab) with enzalutamide for treatment of mCRPC, Guan and colleagues showed that enzalutamide plus ADT significantly enhanced the anti-tumor effect of anti-PD-L1 in animal models compared to enzalutamide plus ADT. These effects were mediated by a direct effect of enzalutamide increasing T cell secretion of IFN- γ and granzyme B. The group demonstrated that the androgen receptor interacts with IFN- γ and granzyme B genes in open chromatin regions (OCRs) of memory CD8 T cells, blocking the rapid production of IFN- γ and Granzyme B enabled by these OCRs upon TCR stimulation. Blocking the androgen-mediated suppression of IFN- γ production in T cells with enzalutamide improved the anti-tumor response elicited by PD-L1 inhibition, helping overcome the relative resistance of prostate cancer to checkpoint inhibitors *in vivo* [8]. Other results corroborate the androgen immune suppressive effects on T cells. ADT increased tumor infiltration of IFN- γ expressing T cells in the prostate TME. Enzalutamide activates IFN- γ signaling pathways and decreases the frequency of immunosuppressive cells in peripheral blood mononuclear cells isolated from patients with mCRPC [25,26]. Our results show a direct effect of AR inhibitors increasing NK cell activation and secretion of IFN- γ , which can also impact T cell function through the functional crosstalk between these two cell lines, enabling an effective anti-tumor response [27]. IFN- γ produced by NK cells promotes an anti-tumor T helper cell type 1 (Th1) polarization in CD4+ T cells [28]. Activated NK cells stimulate CD4+ T cell proliferation by interacting with OX40/OX40L [29] and indirectly influence T cell response by regulating differentiation of dendritic cells. NK cells can induce a type 17 polarization in CD8+ T cells, characterized by the ability to produce IFN- γ and IL-17A through priming of dendritic cells [30]. These findings suggest that therapeutic strategies targeting the activation of CD8 T cells and NK cells could overcome the immune suppressive TME in prostate cancer and lead to meaningful anti-tumor effects. One such strategy could be the combination of AR inhibitors plus monalizumab and anti-PD1/PD-L1 agents. Monalizumab is in clinical development for the treatment of lung cancer and other solid tumors in combination with durvalumab (anti-PD-L1) as a novel strategy to harness the innate immune response and activate NK cells, leading to clinically meaningful tumor response and immune infiltration [13,31,32].

The importance of NK function in PCa and the therapeutic potential of targeting these cells is highlighted by results showing their impact on the clinical outcomes of patients. In a recent pan-cancer analysis, natural killer cell infiltration in PCa tumor specimens was associated with improved OS (HR 0.46, 95% CI 0.38–0.56, $p=0.0001$) [33]. The study also found that NK cell infiltration was associated with a 1.4-2.1-fold increased expression of immunomodulatory receptors LAG3 and TIGIT ($p=0.0001$). Another analysis of a large cohort of tumor specimens of patients with mCRPC showed that tumor infiltration by cytotoxic NK cells and higher expression of activating receptors NKp30 and NKp46 in NK cells isolated from the peripheral blood was associated with improved overall survival and a longer interval to development of castration resistance [34]. Cytokine signaling in the TME, especially IL-6, was associated with resistance to NK cell-mediated cytotoxicity via modulating PD-L1 and NKG2D ligand levels in PCa cells [35]. Peripheral blood NK cell dysfunction was also associated with poor clinical outcomes of PCa and higher disease stage [36]. These findings suggest that modulation of NK cell activation could help overcome and challenge the limited benefit of T cell-centric strategies deployed by PD-1/PD-L1 or CTLA-4 inhibitors for treating mCRPC.

Novel strategies blocking the inhibitory receptor NKG2A expressed on NK and CD8+ cells are under clinical investigation to overcome resistance to anti-PD-1/PD-L1 checkpoint inhibition [37]. NKG2A is an inhibitory checkpoint expressed on the cell surface of CD8, nearly half of circulating NK cells, and can be induced by cytokines such as IL-15 and IL-12 [38,39]. It is a heterodimer, bound with CD94 in humans and mice, and recognizes the non-classical class I major histocompatibility complex (MHC-I) molecules of human leukocyte antigen (HLA)-E. HLA-E expression is present in normal tissue as a protective “self” signaling, and it is up-regulated in various malignancies, including prostate cancer [40,41,42,43]. The inhibitory function on NK cells is mediated through the binding of HLA-E to NKG2A/CD94, leading to the recruitment of the SHP-1 tyrosine phosphatase to the tyrosine-phosphorylated form of the intracytoplasmic tyrosine-based inhibitory motifs (ITIM). When phosphorylated, these motifs recruit phosphatases (SHP-1/2 or SHIP) responsible for transmitting inhibitory signals to immune effector cells. To our knowledge, we describe for the first time that HLA-E expression in prostate cancer cells is modulated by androgen signaling. AR inhibitors enzalutamide and darolutamide increased the expression of HLA-E in androgen-sensitive PCa cell lines. The ARi-driven upregulation of HLA-E could suppress NK cells and the innate immune response and contribute to the cold tumor microenvironment. Even though strategies enhancing NK cell cytotoxicity might display promising results, blocking the immune inhibitory HLA-E/NKG2A axis could result in additional benefits.

The limitations of our results include the lack of results from animal models validating the ARi-induced activation of NK cells and its translation into an *in vivo* anti-tumor effect. There is also limited insight into the mechanisms of androgen receptor regulation of NK cell cytokine production. Whether this is a direct effect mediated by AR on ARE, a post-translational regulation, or is under epigenetic modulation also remains to be further characterized. We also did not investigate the expression of HLA-E in human prostate tumor specimens pre- and post-androgen blockage to validate the observation in PCa cell lines.

These results highlight the potential therapeutic implication of NK-activating strategies for the treatment of prostate cancer. The additive effect of androgen receptor inhibitors and monalizumab (anti-NKG2A) activating NK cells and enhancing PCa cell killing support further investigation of this combination *in vivo* with the potential for immediate clinical translation. Encouraging synergy of durvalumab and monalizumab in ongoing clinical trials for the treatment of lung cancer supports the clinical feasibility of this combination that could be expanded with the addition of androgen receptor inhibitors in advanced prostate cancer as a potential novel platform to modulate the cold TME in prostate cancer.

References

1. Siegel RL, Miller KD, Wagle NS, Jemal A. Cancer statistics, 2023. *CA Cancer J Clin.* 2023 Jan;73(1):17-48. PMID: 36633525.
2. Freedland SJ, Davis M, Epstein AJ, Arondekar B, Ivanova JI. Real-world treatment patterns and overall survival among men with Metastatic Castration-Resistant Prostate Cancer (mCRPC) in the US Medicare population. *Prostate Cancer Prostatic Dis.* 2023 Oct 2. PMID: 37783836.
3. Antonarakis ES, Piulats JM, Gross-Goupid M, et al. Pembrolizumab for Treatment-Refractory Metastatic Castration-Resistant Prostate Cancer: Multicohort, Open-Label Phase II KEYNOTE-199 Study. *J Clin Oncol.* 2020 Feb 10;38(5):395-405. PMID: 31774688.
4. Vitkin N, Nersesian S, Siemens DR, Koti M. The Tumor Immune Contexture of Prostate Cancer. *Front Immunol.* 2019 Mar 28;10:603. PMID: 30984182.
5. Karwacki J, Kiełbik A, Szlasa W, Sauer N, Kowalczyk K, Krajewski W, Saczko J, Kulbacka J, Szydełko T, Małkiewicz B. Boosting the Immune Response-Combining Local and Immune Therapy for Prostate Cancer Treatment. *Cells.* 2022 Sep 7;11(18):2793. PMID: 36139368.
6. Schweizer MT, Ha G, Gulati R, Brown LC, McKay RR, Dorff T, Hoge ACH, Reichel J, Vats P, Kilari D, Patel V, Oh WK, Chinnaiyan A, Pritchard CC, Armstrong AJ, Montgomery RB, Alva A. CDK12-Mutated Prostate Cancer: Clinical Outcomes With Standard Therapies and Immune Checkpoint Blockade. *JCO Precis Oncol.* 2020;4:382-392. PMID: 32671317.
7. Barata P, Agarwal N, Nussenzeig R, Gerendash B, Jaeger E, Hatton W, Ledet E, Lewis B, Layton J, Babiker H, Bryce A, Garje R, Stein C, Kiedrowski L, Saylor P, Sartor O. Clinical activity of pembrolizumab in metastatic prostate cancer with microsatellite instability-high (MSI-H) detected by circulating tumor DNA. *J Immunother Cancer.* 2020 Aug;8(2):e001065. PMID: 32788235.
8. Guan X, Polessio F, Wang C, Sehrawat A, Hawkins RM, Murray SE, Thomas GV, Caruso B, Thompson RF, Wood MA, Hipfinger C, Hammond SA, Graff JN, Xia Z, Moran AE. Androgen receptor activity in T cells limits checkpoint blockade efficacy. *Nature.* 2022 Jun;606(7915):791-796. PMID: 35322234.
9. Kissick HT, Sanda MG, Dunn LK, Pellegrini KL, On ST, Noel JK, Arredouani MS. Androgens alter T-cell immunity by inhibiting T-helper 1 differentiation. *Proc Natl Acad Sci U S A.* 2014 Jul 8;111(27):9887-92. PMID: 24958858
10. Graff JN, Beer TM, Alumkal JJ, Slottke RE, Redmond WL, Thomas GV, Thompson RF, Wood MA, Koguchi Y, Chen Y, Latour E, Bergan RC, Drake CG, Moran AE. A phase II single-arm study of pembrolizumab with enzalutamide in men with metastatic castration-resistant prostate cancer progressing on enzalutamide alone. *J Immunother Cancer.* 2020 Jul;8(2):e000642. PMID: 32616555.

11. Henze L, Schwinge D, Schramm C. The Effects of Androgens on T Cells: Clues to Female Predominance in Autoimmune Liver Diseases? *Front Immunol.* 2020 Jul 29;11:1567. PMID: 32849531.
12. Gubbels Bupp MR, Jorgensen TN. Androgen-Induced Immunosuppression. *Front Immunol.* 2018 Apr 17;9:794. PMID: 29755457.
13. Cho M, Bendell JC, Han S, et al. Durvalumab + monalizumab, mFOLFOX6, and bevacizumab in patients (pts) with metastatic microsatellite-stable colorectal cancer (MSS-CRC). *Annals of Oncology.* 2019. 30 (suppl_5): v475-v532.
14. Cao B, Qi Y, Zhang G, Xu D, Zhan Y, Alvarez X, Guo Z, Fu X, Plymate SR, Sartor O, Zhang H, Dong Y. Androgen receptor splice variants activating the full-length receptor in mediating resistance to androgen-directed therapy. *Oncotarget.* 2014 Mar 30;5(6):1646-56. PMID: 24722067.
15. Kwikas AR, Ardiani A, Gameiro SR, Richards J, Hall AB, Hodge JW. Androgen deprivation therapy sensitizes triple-negative breast cancer cells to immune-mediated lysis through androgen receptor-independent modulation of osteoprotegerin. *Oncotarget.* 2016 Apr 26;7(17):23498-511. PMID: 27015557.
16. Barton VN, D'Amato NC, Gordon MA, Lind HT, Spoelstra NS, Babbs BL, Heinz RE, Elias A, Jedlicka P, Jacobsen BM, Richer JK. Multiple molecular subtypes of triple-negative breast cancer critically rely on androgen receptors and respond to enzalutamide in vivo. *Mol Cancer Ther.* 2015 Mar;14(3):769-78. PMID: 25713333.
17. Mina A, Yoder R, Sharma P. Targeting the androgen receptor in triple-negative breast cancer: current perspectives. *Onco Targets Ther.* 2017 Sep 20;10:4675-4685. PMID: 29033586.
18. Rochette L, Méloux A, Zeller M, Cottin Y, Vergely C. Functional roles of GDF15 in modulating microenvironment to promote carcinogenesis. *Biochim Biophys Acta Mol Basis Dis.* 2020 Aug 1;1866(8):165798. PMID: 32304740.
19. Hoeres T, Holzmann E, Smetak M, Birkmann J, Wilhelm M. PD-1 signaling modulates interferon- γ production by Gamma Delta ($\gamma\delta$) T-Cells in response to leukemia. *Oncoimmunology.* 2018 Dec 14;8(3):1550618. PMID: 30723581.
20. Garnier L, Pick R, Montorfani J, Sun M, Brighouse D, Liaudet N, Kammertoens T, Blankenstein T, Page N, Bernier-Latamani J, Tran NL, Petrova TV, Merkler D, Scheiermann C, Hugues S. IFN- γ -dependent tumor-antigen cross-presentation by lymphatic endothelial cells promotes their killing by T cells and inhibits metastasis. *Sci Adv.* 2022 Jun 10;8(23):eabl5162. PMID: 35675399.
21. Ardiani A, Gameiro SR, Kwikas AR, Donahue RN, Hodge JW. Androgen deprivation therapy sensitizes prostate cancer cells to T-cell killing through androgen receptor-dependent modulation of the apoptotic pathway. *Oncotarget.* 2014 Oct 15;5(19):9335-48. PMID: 25344864.
22. Bonaterra GA, Schleper A, Skowronek M, Kilian LS, Rink T, Schwarzbach H, Heers H, Hänze J, Rexin P, Ramaswamy A, Denkert C, Wilhelm B, Hegele A, Hofmann R, Weihe

E, Kinscherf R. Increased Density of Growth Differentiation Factor-15+ Immunoreactive M1/M2 Macrophages in Prostate Cancer of Different Gleason Scores Compared with Benign Prostate Hyperplasia. *Cancers*. 2022 Sep 22;14(19):4591. PMID: 36230513.

23. Lee N, Llano M, Carretero M, Ishitani A, Navarro F, López-Botet M, Geraghty DE. HLA-E is a major ligand for the natural killer inhibitory receptor CD94/NKG2A. *Proc Natl Acad Sci U S A*. 1998 Apr 28;95(9):5199-204. PMID: 9560253.

24. Wang X, Xiong H, Ning Z. Implications of NKG2A in immunity and immune-mediated diseases. *Front Immunol*. 2022 Aug 10;13:960852. PMID: 36032104.

25. Laccetti AL, Subudhi SK. Immunotherapy for metastatic prostate cancer: immuno-cold or the tip of the iceberg? *Curr Opin Urol*. 2017 Nov;27(6):566-571. PMID: 28825923.

26. Renee N. Donahue, Ravi A. Madan, Jacob Richards, Italia Grenga, Lauren M. Lepone, Christopher R. Heery, James L. Gulley, Jeffrey Schlom; Abstract 4901: Short-course enzalutamide reveals immune activating properties in patients with biochemically recurrent prostate cancer. *Cancer Res* 15 July 2016; 76 (14_Supplement): 4901

27. Portale F, Di Mitri D. NK Cells in Cancer: Mechanisms of Dysfunction and Therapeutic Potential. *Int J Mol Sci*. 2023 May 30;24(11):9521. PMID: 37298470.

28. Alspach E, Lussier DM, Schreiber RD. Interferon γ and Its Important Roles in Promoting and Inhibiting Spontaneous and Therapeutic Cancer Immunity. *Cold Spring Harb Perspect Biol*. 2019 Mar 1;11(3):a028480. PMID: 29661791.

29. Zingoni A, Sornasse T, Cocks BG, Tanaka Y, Santoni A, Lanier LL. Cross-talk between activated human NK cells and CD4+ T cells via OX40-OX40 ligand interactions. *J Immunol*. 2004 Sep 15;173(6):3716-24. PMID: 15356117.

30. Clavijo-Salomon MA, Salcedo R, Roy S, das Neves RX, Dzutsev A, Sales-Campos H, Borbely KS, Silla L, Orange JS, Mace EM, Barbuto JAM, Trinchieri G. Human NK cells prime inflammatory DC precursors to induce Tc17 differentiation. *Blood Adv*. 2020 Aug 25;4(16):3990-4006. PMID: 32841340.

31. Herbst RS, Majem M, Barlesi F, Carcereny E, Chu Q, Monnet I, Sanchez-Hernandez A, Dakhil S, Camidge DR, Winzer L, Soo-Hoo Y, Cooper ZA, Kumar R, Bothos J, Aggarwal C, Martinez-Marti A. COAST: An Open-Label, Phase II, Multidrug Platform Study of Durvalumab Alone or in Combination With Oleclumab or Monalizumab in Patients With Unresectable, Stage III Non-Small-Cell Lung Cancer. *J Clin Oncol*. 2022 Oct 10;40(29):3383-3393. PMID: 35452273.

32. Cascone T, Kar G, Spicer JD, García-Campelo R, Weder W, Daniel DB, Spigel DR, Hussein M, Mazieres J, Oliveira J, Yau EH, Spira AI, Anagnostou V, Mager R, Hamid O, Cheng LY, Zheng Y, Blando J, Tan TH, Surace M, Rodriguez-Canales J, Gopalakrishnan V, Sellman BR, Grenga I, Soo-Hoo Y, Kumar R, McGrath L, Forde PM. Neoadjuvant Durvalumab Alone or Combined with Novel Immuno-Oncology Agents in Resectable Lung Cancer: The Phase II NeoCOAST Platform Trial. *Cancer Discov*. 2023 Nov 1;13(11):2394-2411. PMID: 37707791.

33. Nick Zorko, Justin Hwang, John R Lozada, Hilary Seifert, Andrew Elliott, Milan Radovich, George W. Sledge, Martin Felices, Elisabeth I. Heath, Dave S. B. Hoon, Wafik S. El-Deiry, Jeffrey Miller, and Emmanuel S. Antonarakis. Pan-cancer analysis of natural killer (NK) cell infiltration in human malignancies: Molecular features and clinical implications. *Journal of Clinical Oncology*. 2023. 41:16_suppl, 2563
34. Pasero C, Gravis G, Granjeaud S, Guerin M, Thomassin-Piana J, Rocchi P, Salem N, Walz J, Moretta A, Olive D. Highly effective NK cells are associated with good prognosis in patients with metastatic prostate cancer. *Oncotarget*. 2015 Jun 10;6(16):14360-73. PMID: 25961317.
35. Xu L, Chen X, Shen M, Yang DR, Fang L, Weng G, Tsai Y, Keng PC, Chen Y, Lee SO. Inhibition of IL-6-JAK/Stat3 signaling in castration-resistant prostate cancer cells enhances the NK cell-mediated cytotoxicity via alteration of PD-L1/NKG2D ligand levels. *Mol Oncol*. 2018 Mar;12(3):269-286. PMID: 28865178.
36. Wu J. Could Harnessing Natural Killer Cell Activity Be a Promising Therapy for Prostate Cancer? *Crit Rev Immunol*. 2021;41(2):101-106. PMID: 34348004.
37. André P, Denis C, Soulard C, Bourbon-Caillet C, Lopez J, Arnoux T, Bléry M, Bonnafous C, Gauthier L, Morel A, Rossi B, Remark R, Breso V, Bonnet E, Habif G, Guia S, Lalanne AI, Hoffmann C, Lantz O, Fayette J, Boyer-Chammard A, Zerbib R, Dodion P, Ghadially H, Jure-Kunkel M, Morel Y, Herbst R, Narni-Mancinelli E, Cohen RB, Vivier E. Anti-NKG2A mAb Is a Checkpoint Inhibitor that Promotes Anti-tumor Immunity by Unleashing Both T and NK Cells. *Cell*. 2018 Dec 13;175(7):1731-1743.e13. PMID: 30503213.
38. Mahapatra S, Mace EM, Minard CG, Forbes LR, Vargas-Hernandez A, Duryea TK, Makedonas G, Banerjee PP, Shearer WT, Orange JS. High-resolution phenotyping identifies NK cell subsets that distinguish healthy children from adults. *PLoS One*. 2017 Aug 2;12(8):e0181134. PMID: 28767726.
39. André P, Brunet C, Guia S, Gallais H, Sampol J, Vivier E, Dignat-George F. Differential regulation of killer cell Ig-like receptors and CD94 lectin-like dimers on NK and T lymphocytes from HIV-1-infected individuals. *Eur J Immunol*. 1999 Apr;29(4):1076-85. PMID: 10229073.
40. Kruijff EM, Sajet A, van Nes JG, Natanov R, Putter H, Smit VT, Liefers GJ, van den Elsen PJ, van de Velde CJ, Kuppen PJ. HLA-E and HLA-G expression in classical HLA class I-negative tumors is of prognostic value for clinical outcomes of early breast cancer patients. *J Immunol*. 2010 Dec 15;185(12):7452-9. PMID: 21057081.
41. Seliger B, Jasinski-Bergner S, Quandt D, Stoehr C, Bukur J, Wach S, Legal W, Taubert H, Wullich B, Hartmann A. HLA-E expression and its clinical relevance in human renal cell carcinoma. *Oncotarget*. 2016 Oct 11;7(41):67360-67372. PMID: 27589686.
42. Zeestraten EC, Reimers MS, Saadatmand S, Goossens-Beumer IJ, Dekker JW, Liefers GJ, van den Elsen PJ, van de Velde CJ, Kuppen PJ. Combined analysis of HLA class I, HLA-E, and HLA-G predicts prognosis in colon cancer patients. *Br J Cancer*. 2014 Jan 21;110(2):459-68. PMID: 24196788.

43. Borst L, van der Burg SH, van Hall T. The NKG2A-HLA-E Axis as a Novel Checkpoint in the Tumor Microenvironment. *Clin Cancer Res*. 2020 Nov 1;26(21):5549-5556. PMID: 32409305.

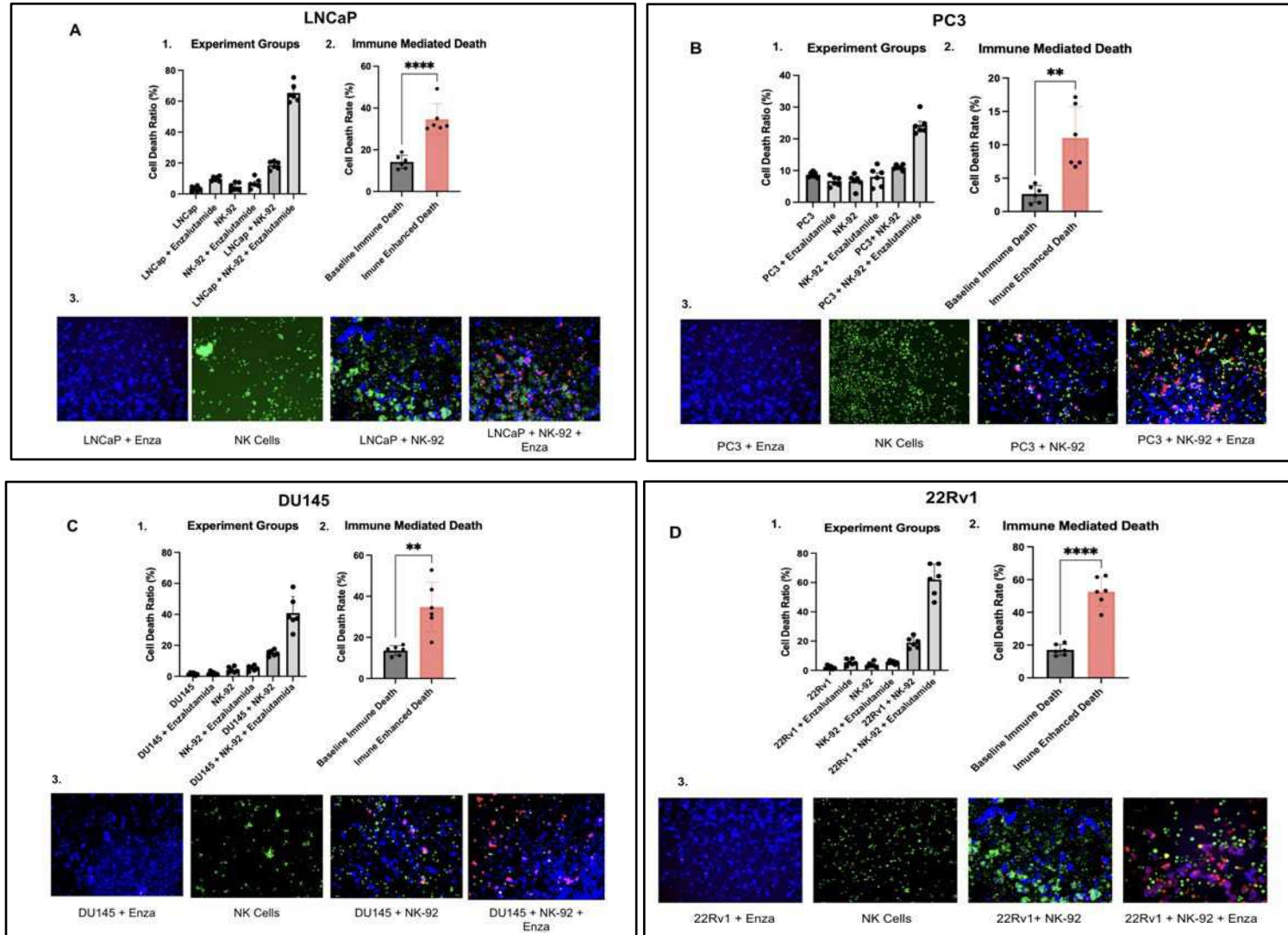


Figure 1. ARi enhances NK-cell killing of PCa cell lines *in vitro*. Results with the PCa cell lines (**A**: LNCaP, **B**: PC3, **C**: DU145, and **D**: 22Rv1) and the NK-92 cell line with or without enzalutamide (10 μ M). Cells were cultured in a 1:1 ratio over 24h. Tumor cells were dyed with CMAC blue dye, and the NK-92 cell line was dyed with CMFDA green dye. The ethidium homodimer red dye (1 μ M) was used to assess live dead cells. Experiments were performed with tumor cells alone and in the presence of enzalutamide to account for drug-induced cell death alone (Experimental Groups **A1**, **B1**, **C1**, and **D1**). Quantifications were performed using Image J. Every co-culture experiment had an NK-92 control condition alone to validate the nontoxicity of enzalutamide on the immune population (data not shown). The enzalutamide dose was non-cytotoxic to the NK-92 cell line (**Supp. Fig. 1**). The immune-mediated effect of NK-92 on the PCa cell lines in the presence of enzalutamide (immune enhancement death) was normalized to baseline immune and tumor cell killing in each condition [(tumor cells + immune cells) - tumor baseline death = baseline immune death] (**A2**, **B2**, **C2**, and **D2**). The results display an increase in immune-mediated NK cell killing of PCa cell

lines, irrespective of AR status or sensitivity to enzalutamide when treated with the ARi (p-value legends as follows: ns $p>0.05$, * $p\leq 0.05$, ** $P \leq 0.01$, $P \leq 0.001$, and **** $P \leq 0.0001$).

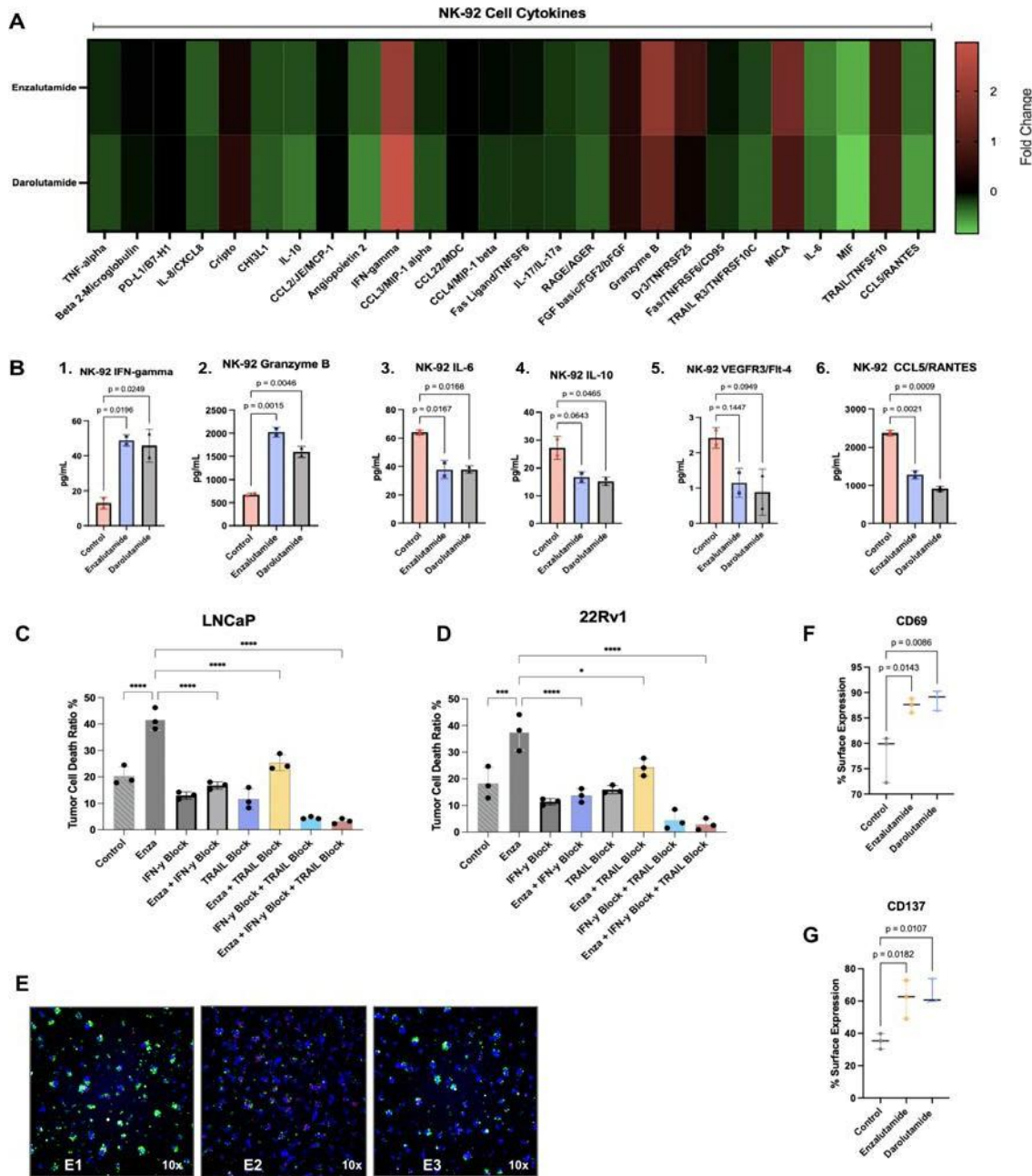


Figure 2. The ARi immune enhancement killing of PCa cell lines by NK-92 cells is dependent on IFN- γ and TRAIL. A: Fold change heat map displaying cytokine changes from the NK-92 cell line alone treated with enza and daro over 24h. **B:** Enza and daro significantly increase the secretion of cytotoxic cytokines from NK-92 cells (**B1, B2**). Enza and daro also reduced the secretion of immunosuppressive cytokines from the NK-92 cell line (**B4** and **B5**). **B5:** NK-92 cell line reduces que T cell chemokine CCL5 when treated with enza or daro. **C** and **D:** IFN- γ blockade reduced the immune enhancement killing of PCa

when treated with enza. The TRAIL blocking mAb (RIK-2) partially reduced the enza immune enhancement effect. The dual blockade of TRAIL and IFN- γ reduces considerably the NK cell cytotoxic killing of PCa cell lines. **E**: Representative images of (**E1**) 22Rv1 + NK-92 (**E2**) 22Rv1 + NK-92 + Enza and (**E3**) 22Rv1 + NK-92 + Enza + IFN- γ block. **F-G**: The immune activation markers, CD69 and CD137, are upregulated when NK-92 cells are treated with ARi (48h). (p-value legend as follows: ns $p>0.05$, * $p\leq 0.05$, ** $P\leq 0.01$, $P\leq 0.001$ and **** $P\leq 0.0001$)

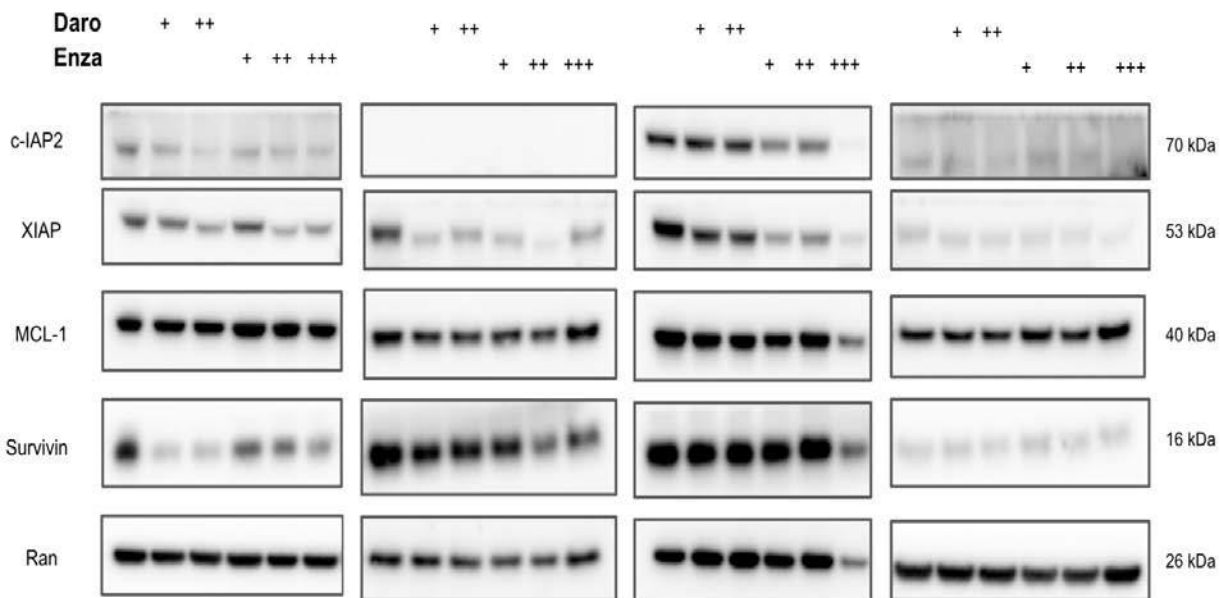
A

LNCap (AR +)

22Rv1 (AR+)

DU145 (AR -)

PC3 (AR-)



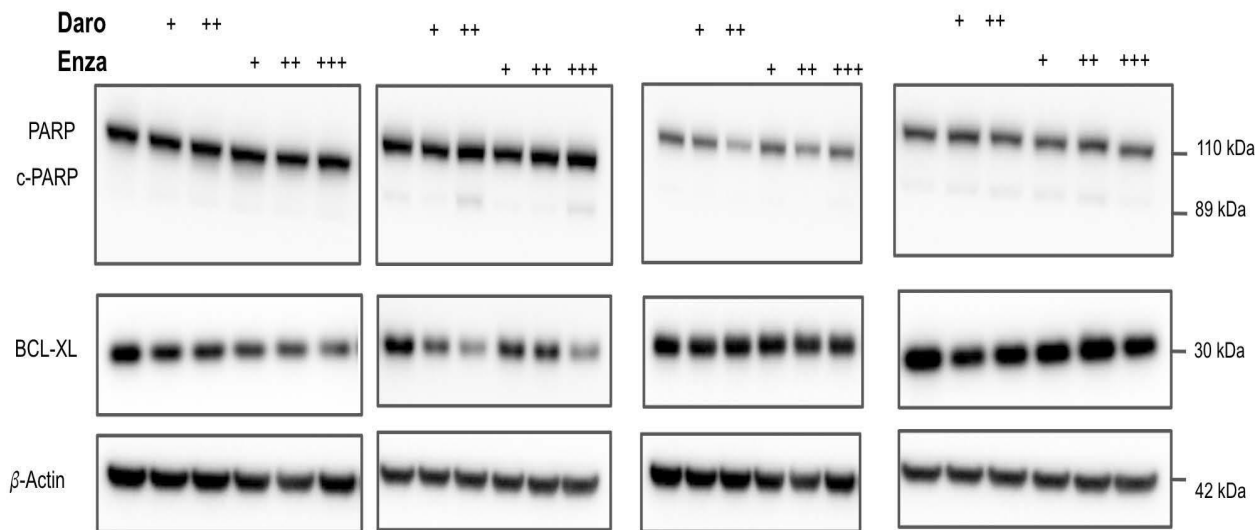
B

LNCap (AR +)

22Rv1 (AR+)

DU145 (AR -)

PC3 (AR-)



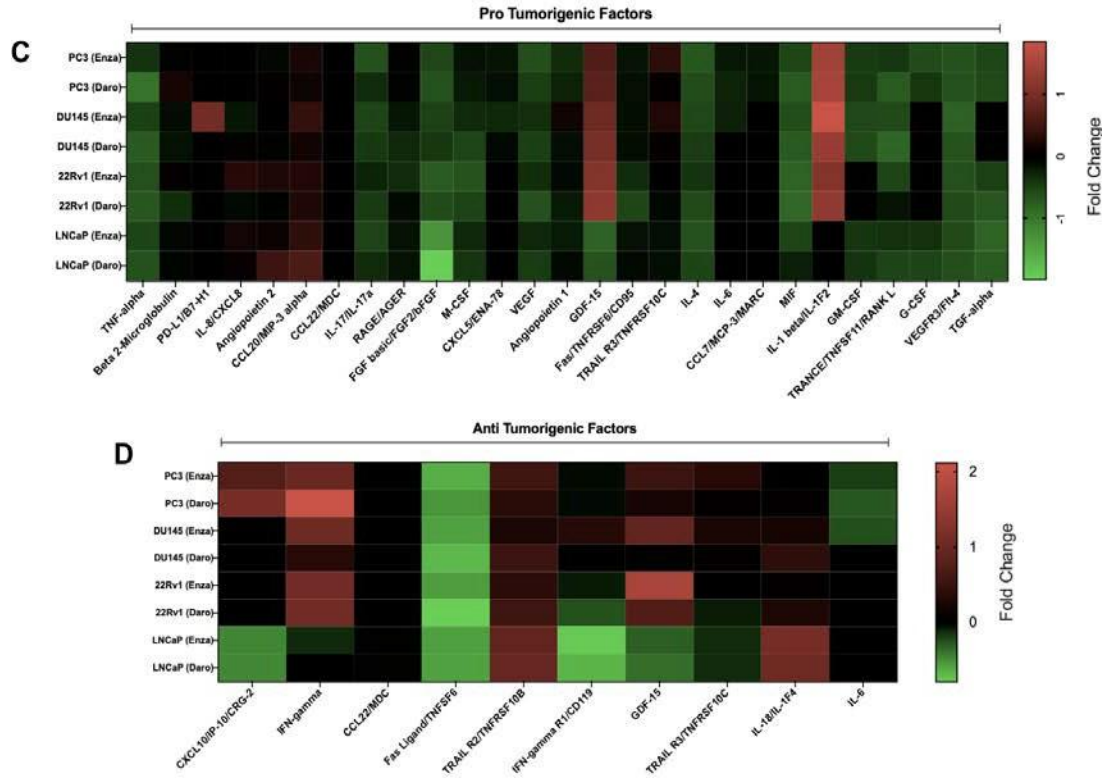


Figure 3. ARI modulates apoptotic and antiapoptotic proteins as well as pro and antitumorigenic cytokines in PCa cell lines. A and B: Western Blot analysis of apoptotic and antiapoptotic proteins on the PCa cell lines with darolutamide (10 and 20 μ M) and enzalutamide (5, 10, 20 μ M) for 48h. Treatment with ARI on the PCa cell lines evidenced changes in both pro and antiapoptotic proteins, irrespective of ARI sensitivity. The changes in protein expression were not similar in the PCa cell lines and cannot explain a single mechanism of tumor cell priming for NK cell killing. **C and D:** PCa cell lines (PC3, DU145, 22Rv1, and LNCaP) were treated with ARI for 24h, and cytokines from the supernatant were analyzed and displayed as a heat map. These tumor-secreting cytokines were collected without the presence of NK cells. Absolute cytokine changes from the PCa cell lines are depicted in **Supp. Fig. 3**.

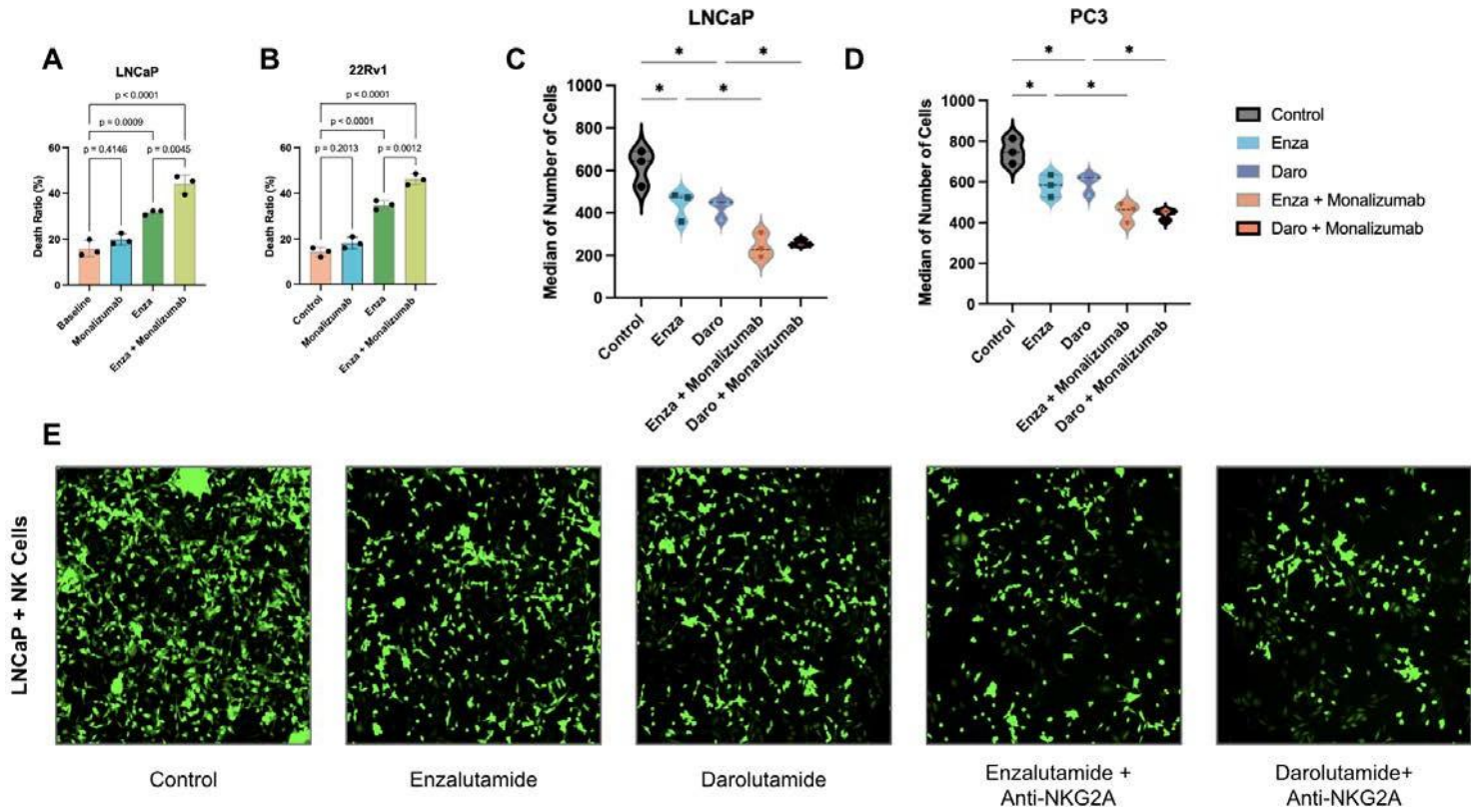


Figure 4. Blocking the NK cell receptor NKG2A with monalizumab potentiates the ARi-induced NK cell activation and killing of PCa cells. PCa cell lines (A: LNCaP and B: 22Rv1) were treated with enzalutamide (10 μ M) and monalizumab in the presence of NK-92 cells (1:1) ratio. Monotherapy with monalizumab, in the fact of NK cells, did not significantly enhance the NK cell killing of PCa cell lines (A and B). ARi and monalizumab significantly improved the NK cell killing of PCa cell lines. C-D GFP- GFP-expressing PCa cells were plated with metastatic castration-sensitive prostate cancer patient-derived NK cells (1:1) ratio. Enza and darolutamide enhanced the killing of the PCa cell lines over 24h. The addition of monalizumab in combination with enza and doro potentiated the killing of PCa. E. Representative images of the GFP-expressing LNCaP cell line co-cultured with patient-derived NK cells and treated with ARi and monalizumab. (P-value legends are as follows: ns p>0.05, * p≤ 0.05, **p ≤ 0.01, p ≤ 0.001, and **** p ≤ 0.0001).

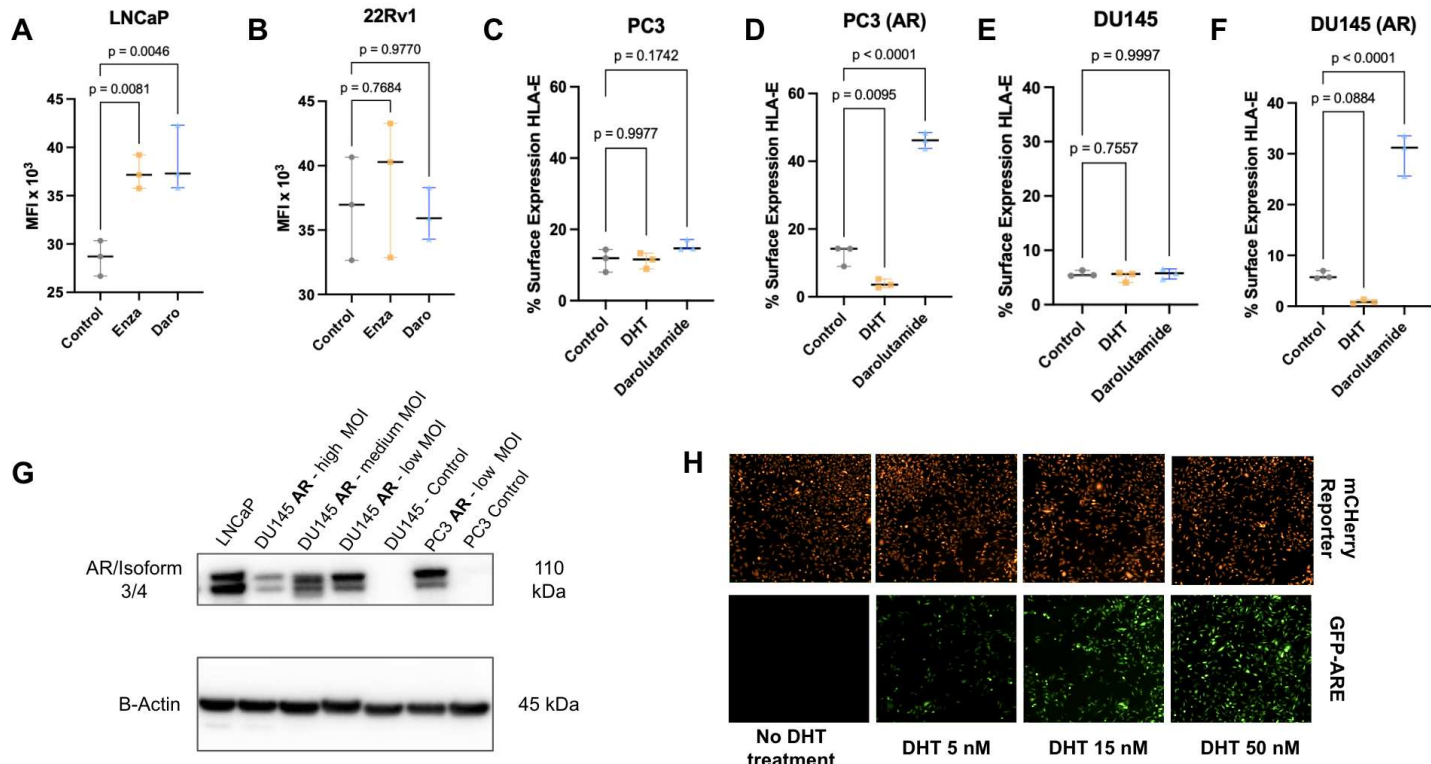


Figure 5. Prostate cancer cells' expression of HLA-E, the ligand of NKG2A, is modulated by androgen signaling. **A:** HLA-E mean fluorescence intensity (MFI) on LNCaP cells treated with enza (15 μ M) and daro (20 μ M) for 48h. **B:** HLA-E MFI of the AR blockade-resistant 22Rv1 cell line treated with enza (15 μ M) and daro (20 μ M) for 48h. To evaluate the AR signaling dependence on the surface expression of HLA-E, the AR negative cell lines (PC3 and DU145) were transduced with AR receptor (**G**) and AR reporter (**H**). The m-Cherry AR transduced reporter expressed on PC3 (**H**) and DU145 cell lines was functionally assessed and exhibited a GFP signal when cells were treated with increasing DHT doses (**H**). **C-D:** The AR-negative cell line (PC3) and the new AR-responsive PC3-AR cell line were evaluated for surface expression of HLA-E upon DHT treatment and ARi with darolutamide. The AR-negative PC3 cell line did not express significant changes in HLA-E surface expression (**C**), but the AR-responsive one (PC3-AR) displayed increased HLA-E upon ARi (**D**). Similar findings were also observed on the DU145 (AR-responsive) cell lines (**E-F**).

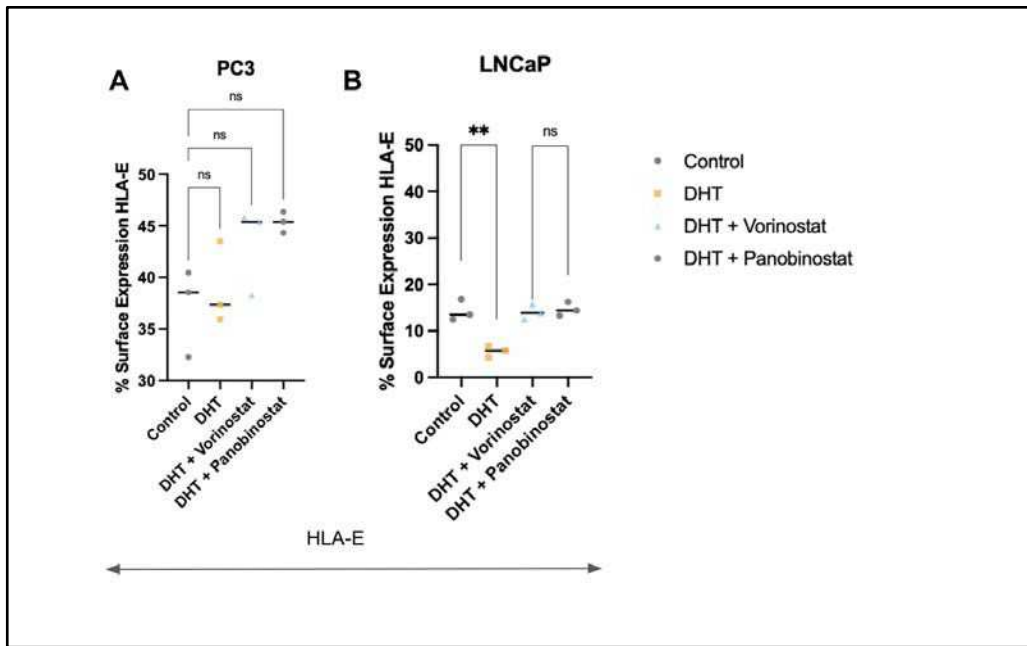


Figure 6. Androgen modulates HLA-E expression through an epigenetic mechanism. The PC3 and LNCaP cell lines were kept in DHT (30 nM) supplemented media for at least five days before experiments. (A-B) Surface expression of HLA-E (48h) was evaluated on the AR-responsive cell lines LNCaP and the AR-non-responsive PC3 cell line after HDACi. HLA-E was also assessed after DHT treatment with and without HDACi. The HDACi vorinostat (0.3 μ M) and panobinostat (3 nM) were used in the experiments. (P- value legends are as follows: ns $p>0.05$, * $p\leq 0.05$, ** $p \leq 0.01$, $p \leq 0.001$, and *** $p \leq 0.0001$).

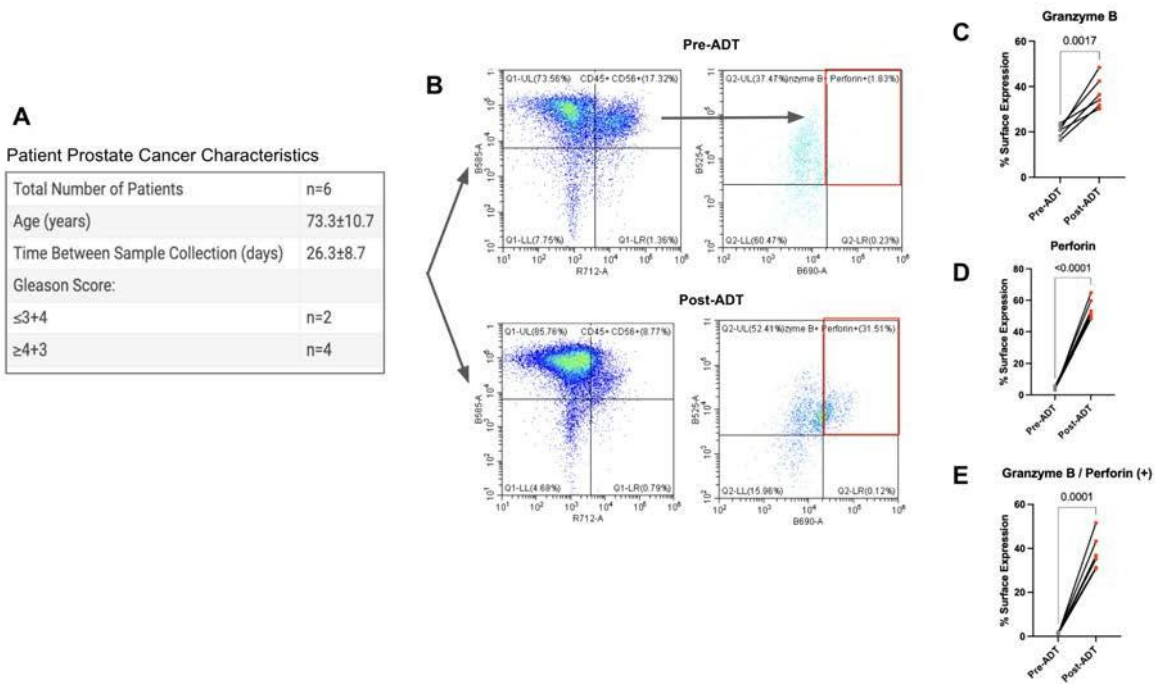
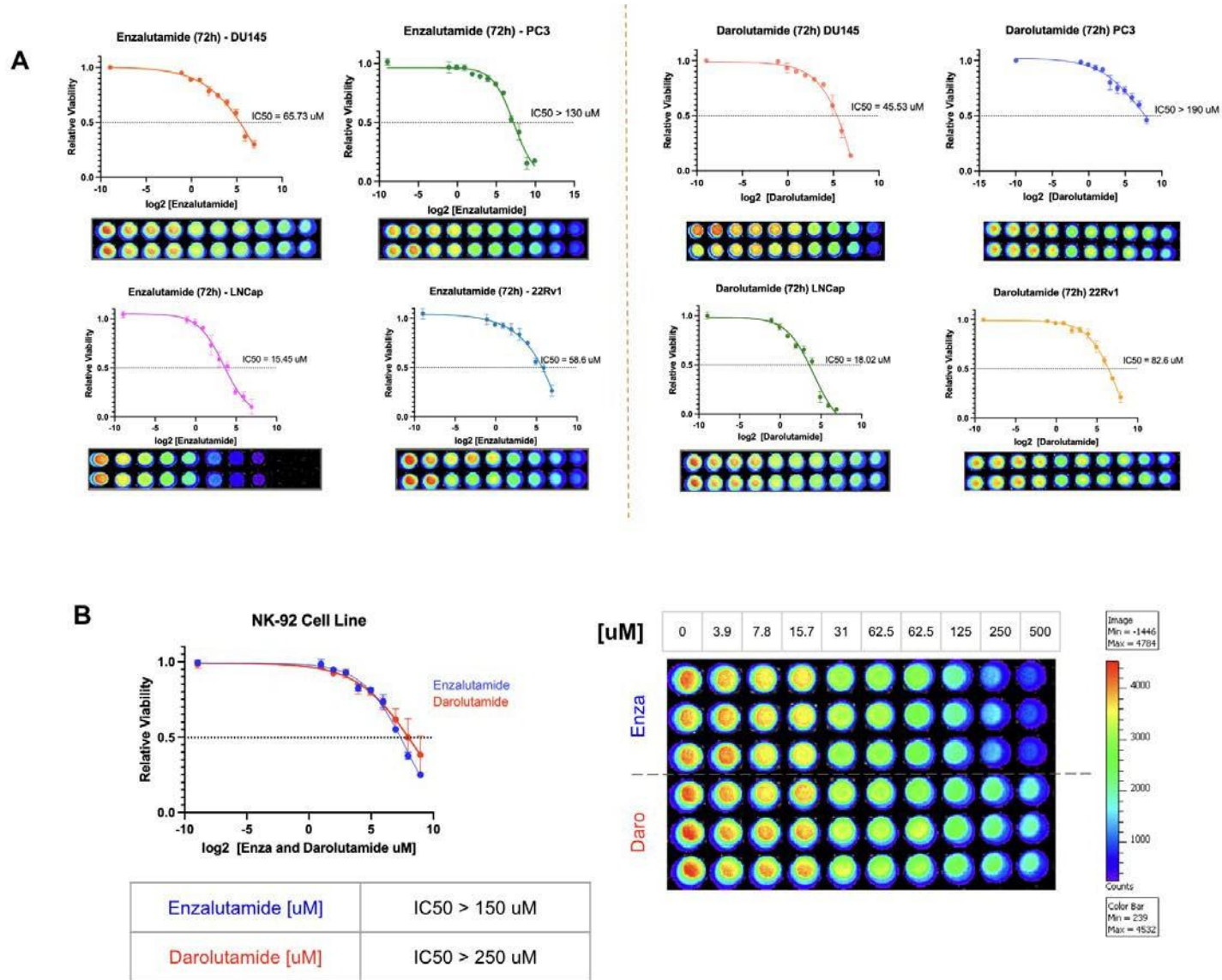


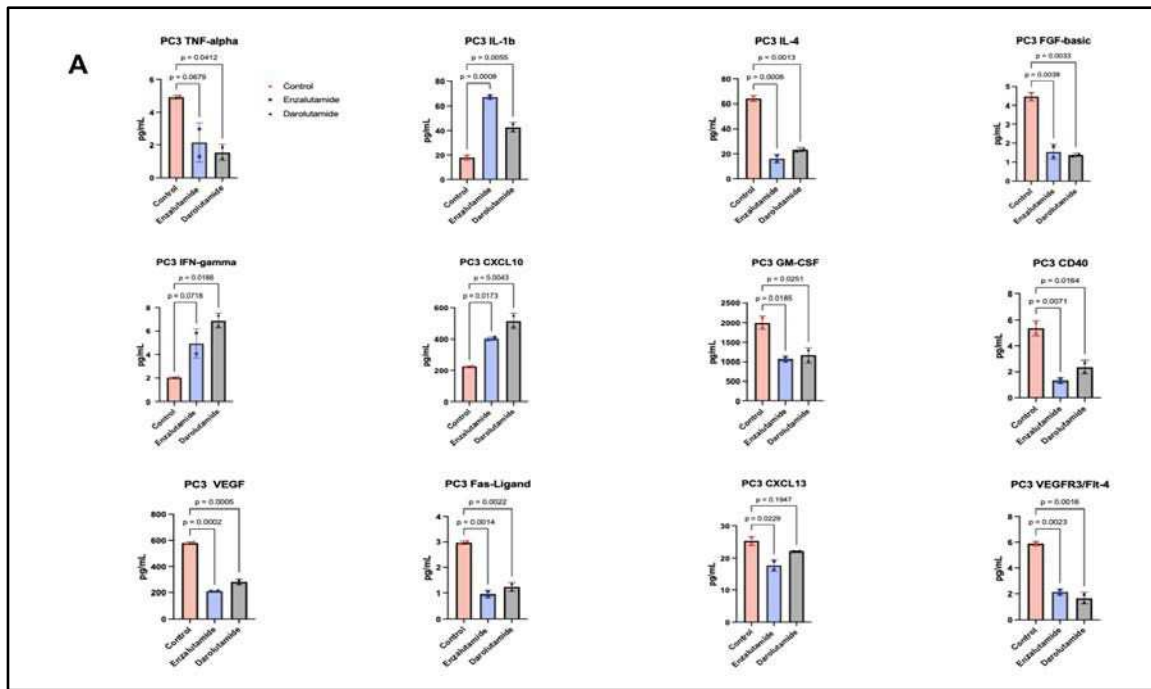
Figure 7. Androgen deprivation therapy (ADT) increases patient-derived NK cell cytotoxic markers. (A) Patient characteristics. Metastatic castration-sensitive prostate cancer patients (n=6) had whole PBMC's and NK cell isolation performed before and after the start of ADT. The activation profile of these NK cells was evaluated by flow cytometry. NK Cells were gated on CD56+CD45 live PBMC population, and a representative matched patient is depicted in **B**. **(C)** Granzyme B, **(D)** Perforin, and double positive population **(E)** displayed increased expression after ADT. A paired t-test was performed, and the results indicate the matched patient cohort (n=6) pre- and post-ADT.

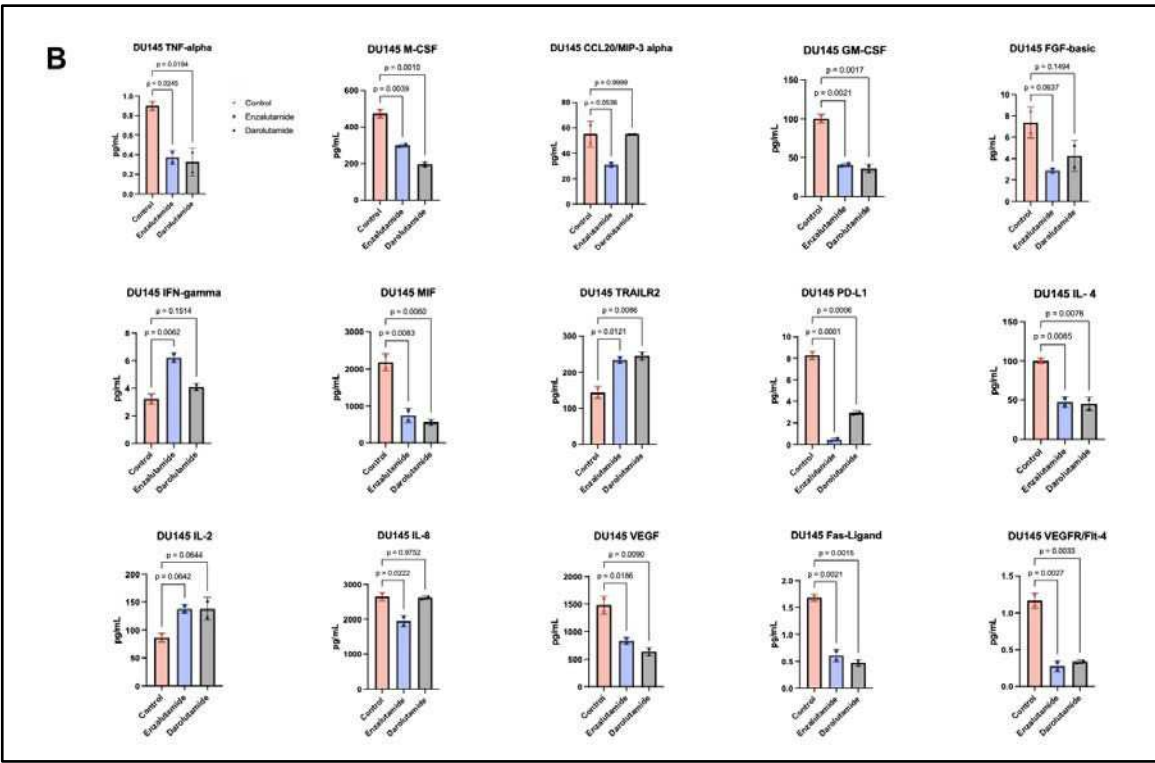
Sup. Fig. 1. Enzalutamide and darolutamide viability assays with prostate cancer cell lines and NK-92 cell line.

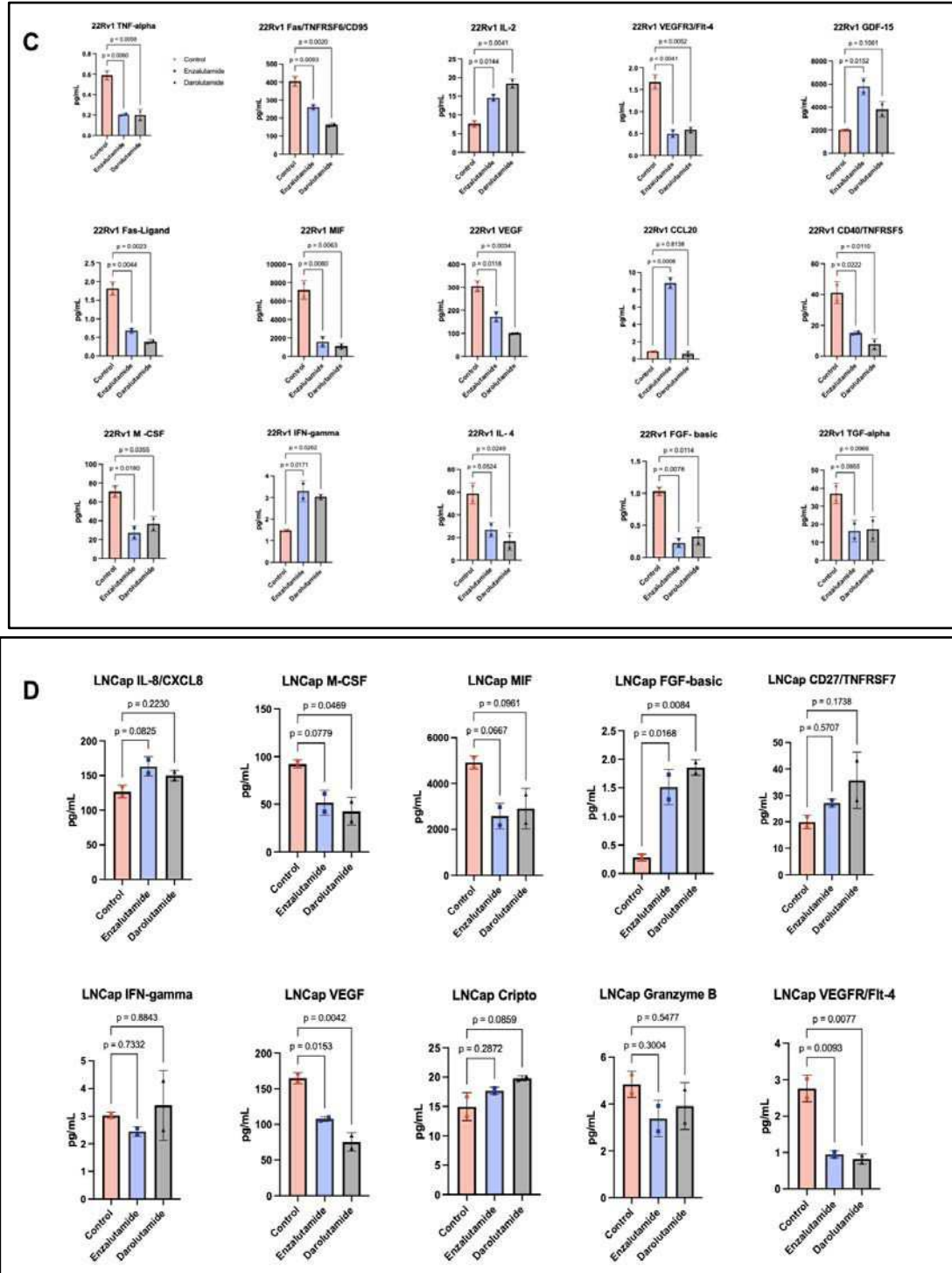


Sup. Fig1. A - Cell Titer Glow (CTG) viability assay of PCa cell lines treated with enzalutamide or darolutamide. Five thousand cells were plated overnight and treated with increasing concentrations of enzalutamide and darolutamide after 24h. Viability assay was performed at 72h and normalized to the control. The IC₅₀ was determined by nonlinear regression. **B** - NK-92 cell line viability was assessed upon enza and darolutamide treatment. Daro and enza displayed nontoxicity on NK-92 cells with doses used in the coculture assays (enza = 10 μM and dero = 20 μM).

Supp. Fig. 2. Cytokine secretion profile of PCa treated with ARi

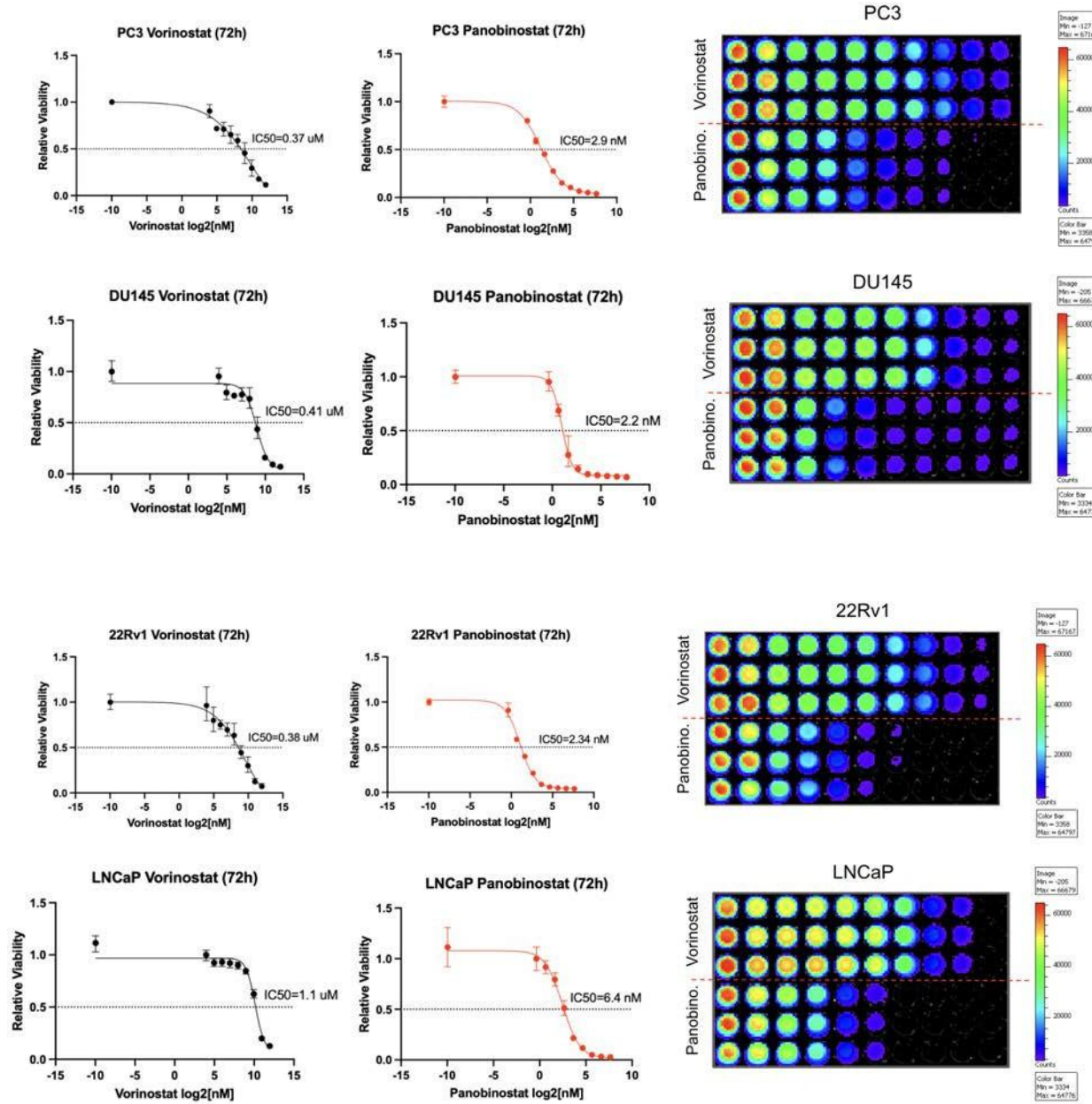






Sup. Fig 2. Individual cytokine analysis from PCa treated with enza and darolutamide after 24h. The PC3 (A), DU145 (B), 22Rv1 (C), and LNCaP (D) cell lines were treated with enza (10 μ M) and daro (15 μ M) for 24h, and the supernatant was collected for cytokine profiling.

Supp. Fig. 3. PCa cell lines viability with pan HDAC inhibitors (Panobinostat and Vorinostat)



Supp. Fig. 3. CellTiterGlo (CTG) viability assay of PCa cell lines treated with panobinostat or vorinostat. Five thousand cells were plated overnight and treated with increasing concentrations of panobinostat or vorinostat after 24h. Viability assay was performed at 72h and normalized to the control. The IC50 was determined by nonlinear regression.